THE SATELLITE BAND PATTERNS IN THE NEAR ULTRAVIOLET ABSORPTION SPECTRA OF ISOTOPIC COMPOUNDS OF ACETALDEHYDE

By

Kim Hok-Kin Ng

B.Sc., B.Sc.

A thesis submitted to the Department of Chemistry in partial fulfillment of the requirements for the degree of Master of Science

Brock University

St. Catharines, Ontario

Sept., 1978

ABSTRACT

TITLE : The Satellite Band Patterns in the Near Ultraviolet Absorption Spectra of Isotopic Compounds of Acetaldehyde

AUTHOR : Kim Hok-Kin Ng

SUPERVISOR : Dr. D. C. Moule

NUMBER OF PAGES : ix , 61

ABSTRACT : The 3700 Å - 3000 Å absorption spectra of CH_3CHO and its isotopic compounds such as CH_3CDO, CD_3CHO and CD_3CDO were studied in the gas phase at room temperature and low temperatures. The low resolution spectra of the compounds were recorded by a 1.5 m Baush and Lomb grating spectrograph. The high resolution spectra were recorded by a Ebert spectrograph with the Echelle grating and the holographic grating separately. The multiple reflection cells were used to achieve the long path length. The pressure-path length used for the absorption spectrum of CH_3CHO was up to 100 mm Hg × 91.43m. The emission spectrum and the excitation spectrum of CH_3CHO were also recorded in this research. The calculated satellite band patterns which were obtained by the method of Lewis were used to compare with the observed near UV absorption spectrum of acetaldehyde. These calculated satellite band patterns belonged to two cases: namely, the barriers-

in-phase case and the barriers-out-of-phase case. Each of the calculated patterns corresponded to a stable conformation of acetaldehyde in the excited state. The comparisons showed that the patterns in the observed absorption spectra corresponded to the H-H eclipsed conformations of acetaldehyde in the excited state. The least squares fitting analysis showed that the barrier heights in the excited state were higher than in the ground state. Finally, the isotopic shifts for the isotopic compounds of acetaldehyde were compared to the compounds with the similar deuterium substitution.

ACKNOWLEDGEMENTS

I wish to acknowledge my indebtedness to my supervisor, Dr. D. C. Moule for his encouragement, his advice and his valuable discussions during the period of this research and thesis preparation.

I would like to thank Dr. E. A. Cherniak for his advice in the emission spectrum part of this experiment and for his permission to use the laboratory facilities in his laboratory.

I also wish to thank Dr. S. M. Rothstein and Dr. W. K. Li for their assistance in INDO and MINDO3 programming.

I would like to thank my colleagues Mrs. C. Lessard and Dr. R. Judge for their friendship and constant helps.

I thank Mr. Paul W. Lee for his literal consultations.

I am grateful to the Ministry of Colleges and Universities for offering me the Ontario Graduate Scholarship and to the Department of Chemistry at Brock University for the financial assistance during the years 1976 to 1978.

Last, but not least, I especially appreciate the encouragement of my wife, Anna Ng, and her understanding.

TABLE OF CONTENTS

LIST OF TABLES

LIST OF FIGURES

Page

CHAPTER 1

INTRODUCTION

Acetaldehyde is isoelectronic with formyl fluoride HFCO. Its excited electronic state is similar to that of formaldehyde H_2CO, so that its electronic transition is the analogue of that in H_2CO. A weak absorption ($\tilde{A} \leftarrow \tilde{X}$) of acetaldehyde vapor between 3500 Å and 2500 Å belongs to the excitation of an electron in the nonbonding orbital to the π^* antibonding orbital[1]. From some previous studies on the acetaldehyde absorption spectrum[2-6] , it has been found that those bands at longer wavelengths have complicated fine structure while those bands at shorter wavelengths are more diffuse.

The assignment of the 0-0 band at 3204 Å by Rao and Rao[5] shows that there is an interval of 1125 cm^{-1} which corresponds to the C-O stretching frequency between the progressions in the spectrum.

The fluoresence spectrum of CH_3CHO was studied by Murad[7]. It was found that the short wavelength emission limit at 3515 Å was very close to the long wavelength absorption limit at 3483 Å . By comparing the absorption and emission curves of CH_3CHO , Innes and Giddings[6] concluded that the origin of the transition was probably at 3484 Å (28700 cm^{-1}) and a 480 cm^{-1} interval was assigned to the aldehyde hydrogen out-of-plane mode.

By using the Herzberg-Teller theory, Worden[8] studied the effect of deuterium substitution on the intensity of the $n \rightarrow \pi^*$ transition in acetaldehyde and found that the intensity change with isotopic substitution was roughly proportional to the change in vibrational frequency. Moreover , Worden concluded that the change in intensity of the $n \rightarrow \pi^*$ transition was a result from the mixing of electronic states by the vibrations which involved either the aldehyde hydrogen (deuterium) out-of-plane bending vibration or the combination of this vibration with some other vibrational modes.

Acetaldehyde is an asymmetric rotor molecule. The molecule exhibits not only an overall rotation and vibration, but also an internal rotation. The methyl group of the molecule rotates with respect to the CHO group about an axis lying on the single plane of symmetry. The axis of the internal rotation is the same as the symmetric axis of the methyl group. This internal rotation is hindered by a threefold potential barrier of 1.16 Kcal / mole.[10]

Several people have attemped to determine the torsional barrier of CH_3CHO[9-12]. Two methods have been used successfully for this purpose. The first one is a microwave splitting-intensity method. The second method is to directly observe the torsional transitions in the far-infrared region. Both methods generate similar values of the barriers to internal rotation of methyl group for CH_3CHO and its isotopic

compounds[11]. To ultilize these methods, it is necessary to know certain parameters of the molecules, such as the principal moments of inertia, the moment of inertia of the methyl group about its axis of symmetry, and the direct cosines of the methyl group symmetric axis with respect to the principal axis.

Lewis et al[13] developed a computer program to determine the energy levels of molecules which have a periodic potential function of the form $V=\frac{1}{2}\Sigma V_n$ (1-COS nØ) . The transition energies and the relative intensities of certain transitions were obtained from this program by inputing values of the reduced rotational constant and the potential barrier height. A satellite band pattern for the internal rotation was formed by plotting the values of intensities against the values of transition energies.

Gorden et al[14] studied the $n\rightarrow\pi^*$ transition from the 6900 Å absorption spectrum of CF_3NO at various temperatures. By using the method of Lewis, Gorden compared the observed and the calculated satellite band structures in this absorption system and found that those band structures were well matched when the barriers were assumed to be out of phase with respect to each other. Hence, Gorden concluded that this electronic excitation ($n\rightarrow\pi^*$) was accompanied by the conformational changes which included the change in the phase of the barrier to internal rotation.

Since both CH_3CHO and CF_3NO belong to the C_s group and the internal rotational barrier of CH_3CHO is not large enough to stabilize the different conformations which are formed by the torsional motion , the conformational changes of CH_3CHO are expected to be active in the $n \rightarrow \pi^*$ transition. The weak absorption of CH_3CHO mentioned above should involve transitions between the torsional levels in the two electronic states.

The objectives of this research are to compare the observed satellite band pattern in the near ultraviolet absorption spectrum of CH_3CHO with a calculated pattern which is adapted from Lewis's method and to study the effect of deuterium substitution on the appearance of the absorption spectra.

CHAPTER 2

THEORETICAL

(A) Torsional Barrier Height , V_3

According to the theory described by Durig, Craven and Harris [15] , the potential energy of the internal rotation about a single bond is a periodic function of the angle of rotation. The symmetric top (CH_3) of acetaldehyde has a single threefold symmetric axis and thus the potential function can be written as

$$V(\phi) = \tfrac{1}{2} V_3 (1 - \cos 3\phi) + \tfrac{1}{2} V_6 (1 - \cos 6\phi) + \cdots (1)$$

,where ϕ is the angle of rotation , V_3 is the height of the threefold barrier , and V_6 is the sixfold term. The value of V_6 is very small when compared with V_3 . The potential function is then adequately represented by the first term only.

$$V(\phi) = \tfrac{1}{2} V_3 (1 - \cos 3\phi) \qquad (2)$$

The Hamiltonian, $\mathcal{H}$, written by Herschbach [12] is represented by the following equation :

$$\mathcal{H} = \mathcal{H}_r + F (p - P)^2 + V(\phi) \qquad (3)$$

The first term, $\mathcal{H}_r$, in equation (3) is the Hamiltonian for the rigid rotor and is expressed by equation (4).

$$\mathcal{H}_r = A P_x^2 + B P_y^2 + C P_z^2 \qquad (4)$$

Equation (4) involves the components of the total angular momenta such as P_x, P_y and P_z along the principal axes and the rotational constants such as A , B and C. In the second term in equation (3) ,F is the internal rotation constant and

is expressed by equation (5)

$$F = \tfrac{1}{2} (\lambda^2 / I_r) \qquad (5)$$

where I_r is the reduced moment of inertia for the relative motion of the two groups. I_r can be calculated from equation (6) ,

$$I_r = I_\alpha (1 - \sum_i \lambda_i^2 I_\alpha / I_i) \qquad (6)$$

where I_α is the moment of inertia of the methyl group about its symmetric axis , I_i is the moment of inertia of the whole molecule about its principal axis and λ_i is the direction cosine between the top axis and the principal axis.

The operator (p - P) in the second term of equation (3) is the relative angular momentum of the top and the frame. If the cross term -2FpP is neglected and the term FP^2 is combined into $\mathcal{H}_r$, the Hamiltonian for the torsional motion, $\mathcal{H}_t$, is separated and represented by equation (7) ,

$$\mathcal{H}_t = Fp^2 + \tfrac{1}{2} V_3 (1 - \cos 3\phi) \qquad (7)$$

When equation (7) is substituted into the Schrödinger wave equation for one dimension, the wave equation becomes

$$F \frac{d^2\psi(\phi)}{d\phi^2} + (E - \tfrac{1}{2} V_3 (1 - \cos 3\phi)) \psi(\phi) = 0 \qquad (8)$$

Equation (8) is compared with the Mathieu equation ,

$$\frac{d^2 Y}{d X^2} + (b - s \cos^2 X) Y = 0 \qquad (9)$$

where b is an eigenvalue of the Mathieu equation and s is a dimensionless parameter of the Mathieu equation.

These two equations can be transformed into one another by substituting their variables :

$$Y = \psi(\phi)$$

$$2X = 3\phi + \pi$$

$$b = 4/9 \ (E/F)$$

$$s = 4/9 \ (V_3 / F) \qquad (10)$$

The energy levels for hindered rotation are

$$E = (9/4)Fb \qquad (11)$$

Both E and b are governed by the torsional quantum number v and the sublevel index σ , so that these paremeters can be writtern as $E_{v\sigma}$ and $b_{v\sigma}$.

The energy level for each torsional quantum number v gives two sublevels. One of these is the non-degenerate A level having the value of σ which equals zero , and the other is the doubly degenerate E level having the value of σ which equals $\pm$ 1 .

The observed infrared frequency corresponding to the transition between two energy levels is calculated by equation (12).

$$\Delta E_{v\sigma} = 9/4 \ F \ \Delta \ b_{v\sigma} \qquad (12)$$

If $\Delta b_{v\sigma}$ is obtained by equation (12) then the value of s can be obtained from the table of solutions [21] from the Mathieu equation (9). The barrier height can then be calculated by using equation (13).

$$V_3 = (9/4)\ Fs \qquad (13)$$

(B) Torsional Energy Levels and Wave Functions

By using the method of J.D. Lewis[13], the internal rotation constant F is expanded into a series

$$F = F_0 + F_3 \cos 3\phi + F_6 \cos 6\phi + \ldots \qquad (14)$$

For the convenience of calculation, the wave equation (8) in part (A) is divided by the first term F_0 in equation (14), while V_6 , F_3 and the other higher order terms are set to zero, with the Hamiltonian for torsional motion becoming :

$$\mathcal{H}_t = -\frac{d}{d\phi}\left(1 + (F_3/F_0)\cos 3\phi \right)\frac{d}{d\phi} + (1/2F_0)\ V_3(1 - \cos 3\phi) \qquad (15)$$

The eigenvalue for the wave equation such as $\mathcal{H}_t\psi(\phi) = \lambda\psi(\phi)$ is given by $\lambda = E_{v\alpha} / F_0$.

The Hamiltonian matrix for equation (15) can be set up in the basis set of equations. In the case of free rotor, the basis set is represented by

$$\psi_m(\phi) = (2\pi)^{-1/2}\ e^{im\phi} \quad , \text{where} \quad m = 0, \pm 1 , \ldots \qquad (16)$$

and it can be transformed into the sine and cosine basis sets by using the Wang[27] transformation.

The matrix is then factored into three blocks, according to the symmetry species α .

If NB is the number of basis functions and v is the torsional quantum number, the basis functions are represented

as follow :

for odd a_1 levels (A COS Block)

$$\psi_{v,a_1} = \sum_n a_{nv} \text{ COS } n \phi \qquad v = 0,2, \ldots. \quad n = 0,3,6,\ldots \tag{17}$$

for odd a_2 levels (A SIN Block)

$$\psi_{v,a_2} = \sum_n b_{nv} \text{ SIN } n \phi \qquad v = 1,3, \ldots \quad n = 3,6, \ldots \tag{18}$$

and for even e levels

$$\psi_{v,e} = \sum_n c_{nv} \text{ COS } n \phi \qquad v = 0,1,2,.. \quad n = 3,6,12,15,.. \tag{19}$$

The element of the NB×NB Hamiltonian matrix is calculated by using equation (20) .

$$H_{kl} = \int \psi_k^* \mathcal{H}_t \psi_l \, d\phi \tag{20}$$

The diagonalization of the resulting matrix yields both eigenvalues and eigenvectors for the wave function.

(C) Selection Rules for the Electronic Transition

The selection rules for electronic transitions are

$a_1 \leftrightarrow a_1$ $\qquad$ $a_1 \not\leftrightarrow a_2$

$a_2 \leftrightarrow a_2$ $\qquad$ $a_1 , a_2 \not\leftrightarrow e$

$e \leftrightarrow e$

The transitions are labelled by $v' - v''$ and A or E is for $a \leftrightarrow a$ or $e \leftrightarrow e$.

(D) Intensities

The transition intensities are calculated by multipying the Frank-Condon factor by the appropriate Boltzman factor.

The Frank-Condon factor is represented by equation (21),

$$\text{Frank-Condon factor} = \left(\langle \psi' | \psi'' \rangle \right)^2 \qquad (21)$$

where ψ'' and ψ' are the wave functions for ground state and excited state respectively.

The Boltzman factor is represented by equation (22),

$$\text{Boltzman factor} = \text{Exp} \left(- E'' / kT \right) \qquad (22)$$

where E'' is the energy difference in the ground state, k is the Boltzman constant and T is the absolute temperature.

CHAPTER 3

EXPERIMENTAL

(A) Reagents

CH_3CHO - Reagent grade acetaldehyde was obtained from BDH chemical Ltd.

CH_3CDO , CD_3CHO , CD_3CDO - The isotopic compounds in 1-gram bulbs were obtained from Merck Sharp and Dohme Canada Ltd.

(B) Apparatus

(a) Sample Cell

1. 2 m Multiple Reflection Cell :

This cell is 2 m long and 10 cm in diameter. Its optical system is similar to that described by White[16]. The low temperature control system is also constructed with the cell. In this system , the multiple reflection cell is surrounded by an insulated jacket. Liquid nitrogen is used as the coolant and is contained in a dewar. The liquid nitrogen is forced through the rubber tubing to a copper manifold and is distributed uniformly along the inner wall. The flow rate of the coolant is controlled by a mercury bubbler. The temperature of the system is measured by using a copper-constantan thermocouple which is attached to a potentiometer. The low temper-

ature system of the multiple reflection cell is illustrated in Fig 1 . The detailed description can be found in the paper published by Biernacki , Moule and Neale[17] .

2. 20 foot White Type Multiple Reflection Cell

This cell is 20 feet long and 6 inches in diameter and is made of aluminium. Its optical system is similar to that for the 2 m multiple reflection cell. The focussing screws are constructed at the outside of the cell .

3. T - Shaped Emission Cell

This T - Shaped cell is 1 inch in diameter. The length of the longer (horizontal) side of the cell is 10 in and the length of the shorter (vertical) side is 5 in. There are 3 plane quartz windows attached to 3 sides of the cell.

(b) Light Source

1. 450 Watt Xenon Arc Lamp (Model c-60-50)
-made by Oriel Optical Corp., Stamford, Conn.
2. 1000 Watt Xenon Arc Lamp (Model BF-1000-13)
-made by Christrie electric Corp., Los Angeles, Calif.
3. 250 Watt Xenon-Mercury Arc Lamp (Model C-72-20)
-made by Oriel Optics Corp, Stamford, Conn.

Fig. 1 The Low Temperature System of 2 m Multiple Reflection Cell

1 - Mirror

2 - Adjusting Screw

3 - Clamp

4 - Cell

5 - Steel Inner Wall

6 - Wooden Outer Box

7 - Polyurethane Foam

8 - Thermocouple

9 - Rubber Tubing

10 - Copper Manifold

11 - Mercury Bubbler

12 - Dewar of Liguid Nitrogen

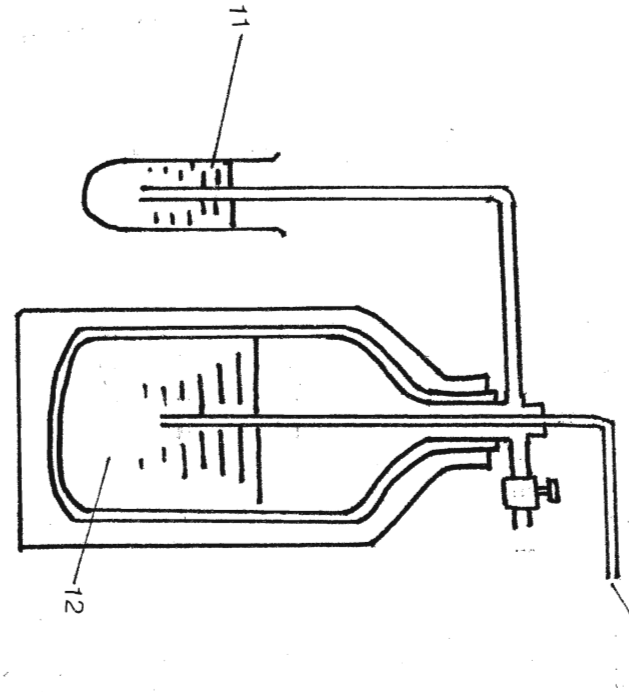
11
12
9

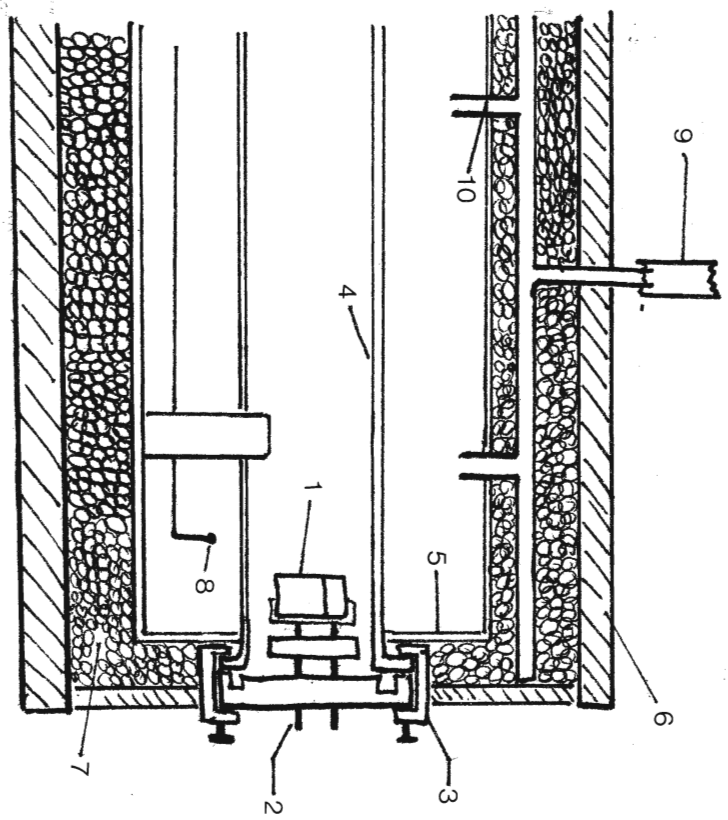
9
10
4
1
8
5
6
7
2
3

(c) Spectrograph

1. 1.5 m Baush and Lomb Grating Spectrograph

The length of this spectrograph is 1.5 m . Its grating has a size of 76.2 mm×38.1 mm and is ruled with 450 grooves per mm. The range of this spectrograph is 1850 Å - 3700 Å in 2 nd order and 3700 Å - 7400 Å in the first order. Its dispersion is 7.5 Å / mm and its resolving power is 70,000 in 2 nd order.

2. Ebert Grating Spectrograph

The Ebert grating spectrograph has a focal length of 20 ft. The aperture for this spectrograph is f/47 (with Echelle grating). Two kinds of grating have been used with this spectrograph. The first one is an Echelle grating and the second one in an holographic grating. The description of the gratings is as follows :

i. Echelle grating -

The model number of this grating is NO.35-53-32-45. The grating has a size of 128 mm × 256 mm and is blazed at 63° 26′ . The number of grooves per mm on the grating is 300. The resolving power of the Ebert spectrograph using this grating is in excess 400,000 in 17 th order. The dispersion of the spectrograph is 0.065 Å /mm.

ii. Holographic grating -

This grating was obtained from J.Y. Optics Ltd. Its area is 110 mm × 110 mm and the number of grooves per mm is 4000. The resolving power of the Ebert spectrograph by using this grating is 300,000.

3. 1 m Czerny-Turner Spectrograph (model 78-460)

This spectrometer is made by the Jarrell-Ash company. The focal length of this spectrometer is one meter. Its grating has an area of 102 mm × 102 mm which is ruled with 1180 grooves/mm. The aperture of this spectrometer is f/8.7 and its dispersion is 8.2 Å/mm in the first order. The Jarrell-Ash recording electronic system (model 82-110) is used to record the signals which are detected by the photomultipier at the exit slit of the spectrometer.

4. 0.25 m Ebert Monochromator (model 82-410)

This monochromator is made by the Jarrell-Ash company. Its focal length is 0.25 m and its aperture is f/3.6 . Its grating has a size of 64 mm × 64 mm and is ruled with 1180 grooves/mm, and is blazed at 3000 Å . Its dispersion is 33 Å / mm.

(C) Procedure

(a) The Low Resolution Absorption Spectrum of Acetaldehyde at Room Temperature

The vapour of CH_3CHO was purified by bulb to bulb distillation on the vacuun line and was transferred directly to the 2 m multiple reflection cell. The light path length for the multiple reflection was selected at 64 m. The spectrum was photographed by the 1.5 m Baush and Lomb grating spectrograph. The slit of the spectrograph was set at 30μ. Kodak spectrum analysis SA NO. 1 film was used to record the second order spectrum. The iron emission lines were used as wavelength standards by recording the light from the hollow cathode lamp on top of the spectrum. The range of the spectrum corresponding to the various vapour pressures are shown in Table 1. The absorption spectra of the isotopic compounds such as CH_3CDO, CD_3CHO and CD_3CDO were recorded by using the same procedure as for CH_3CHO, except without further purification.

The long path length and low resolution absorption spectrum of CH_3CHO was obtained with

the 1.5 m Baush and Lomb grating spectrograph by using the 20 ft White type multiple reflection cell. The vapour pressure of CH_3CHO in the cell was 100 mm Hg and the path length was 91.43 m.

Table 1

Spectrum Range v.s. Vapour Pressure of CH_3CHO

Range (Å)	Vapour Pressure (mm Hg)
3700 - 3554	200
3554 - 3515	100
3515 - 3460	50
3460 - 3427	28
3427 - 3369	10
3369 - 3310	5
3310 - 3250	2
3250 - 3216	1
3216 - 3000	0.5

(b) The Low Resolution Absorption Spectrum of Acetaldehyde at Low Temperatures

The apparatus in this part was as same as that described in part (a). The low temperature control system was added and the temperature was adjusted to change from -53°c to -85°c . The temperature of the system covering the range from 3700 to 3000 Å was shown in Table 2.

The procedures for the isotopic compounds such as CD_3CHO and CD_3CDO were similiar to that for CH_3CHO.

Table 2

Spectrum Range v.s. Temperature in the system for CH_3CHO

Range (Å)	Temperature (°c)
3700 - 3427	- 53
3427 - 3369	- 62
3369 - 3310	- 75
3310 - 3000	- 85

(c) <u>The High Resolution Spectrum of Acetaldehyde at Room Temperature</u>

1. The 17 th order absorption spectrum of CH_3CHO was recorded with the 20 ft Ebert spectrograph. The grating of the Ebert spectrograph was an Echelle grating and a silica prism was used as the order sorter. The reading from the rotatary table of the prism was 16.32 . The slit width of the spectrograph was set at 20μ . The grating was rotated from the counter reading 427 to 460 in order to cover the range from 3300 Å to 3500 Å . A one meter long, one inch diameter absorption cell with quartz windows at both ends was used to acheive a one meter pathlength. The 2 m multiple reflection cell was used to change the path length from 2 m to 8 m. The dispersion of the spectrum was 0.065Å/mm.

2. The first order high resolution absorption spectra of CH_3CHO and its isotopic compounds such as CH_3CDO, CD_3CHO and CD_3CDO were recorded on the 20 ft Ebert spectrograph with the holographic grating. The 2 m multiple reflection cell was used and the pathlength of 64 m was

selected. The vapour pressures of all acetaldehyde compounds were 30 mm Hg. The dispersion of the spectrum was 0.034 Å/mm.

(d) The Emission Spectrum of CH_3CHO

The T-shaped sample cell was used to contain the CH_3CHO vapour in this procedure. The CH_3CHO vapour was allowed to flow through the cell by distilling liquid CH_3CHO from a bulb through the vacuum line and condensing the vapour in another bulb which was surrounded by dry ice. The 250 Watt mercury-xenon arc lamp was used as the light source. The light from the lamp went through the 0.25 m Ebert monochromator in such a way that only the light with wavelength of 3200 Å was transmitted. The monochromatic light excited the CH_3CHO vapour and emission occured. The fluorescence was detected by the 1 m Czerny-Turner spectrometer at a direction perpendicular to the direction of the mercury light.

The set-up is illustrated in Fig 2.

The green fluorescence was obtained when a static system of CH_3CHO was used. It proved to be the fluorescence of biacetyl [18,7]. The fluorescence of CH3CHO in the flow system was light blue. The vapour pressure of CH_3CHO was maintained at 100 mm Hg. The slit width was 400 μ. The spectrum was recorded in the range from 3100 Å to 3800 Å with a scanning

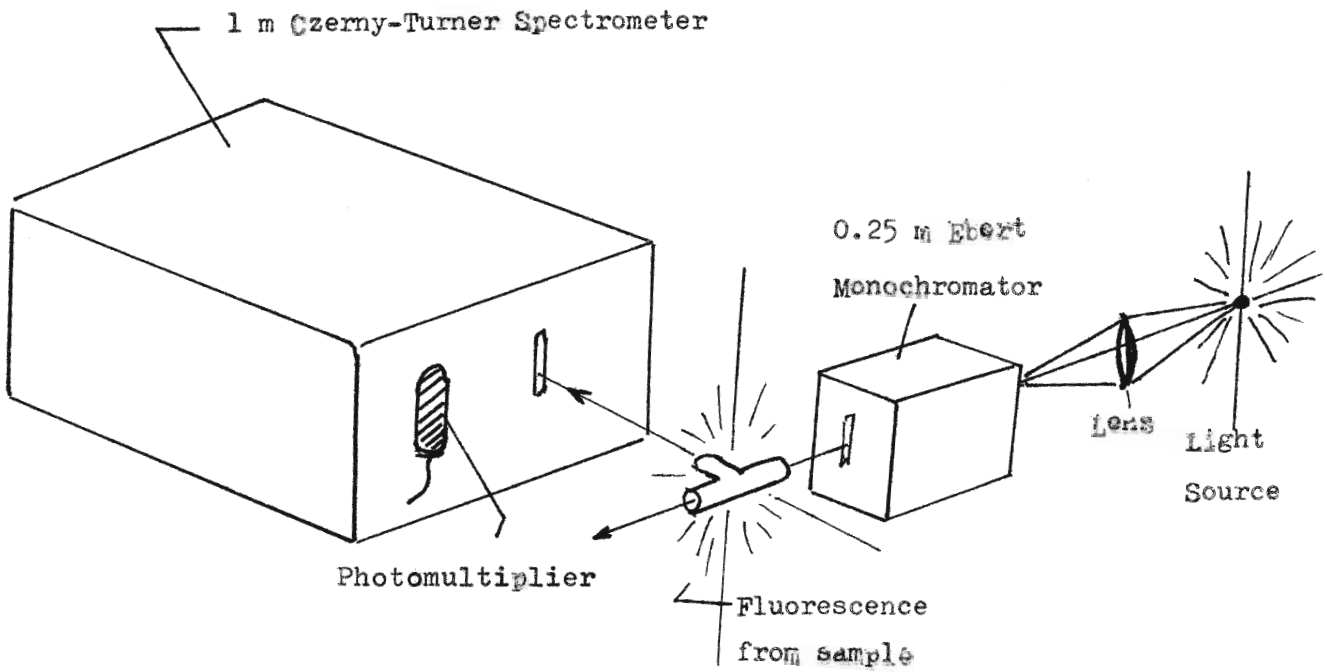
1 m Czerny-Turner Spectrometer
0.25 m Ebert
Monochromator
Lens
Light
Source
Photomultiplier
Fluorescence
from sample

Fig. 2 The Basic Features for the Emission Apparatus.

speed 25 Å/min. The voltage of the photomultiplier was 800 volts. The emission lines from a mercury pen ray lamp were used as the wavelength standard to calibrate the wavelength readings from the recorder.

(e) <u>The Excitation Spectrum of CH_3CHO</u>

The T-shaped cell was used and contained 100 mm Hg pressure of CH_3CHO. The 1000 watt xenon arc lamp was used as the light source. The light was sent into the Czerny-Turner spectrometer, and the transmitted monochromatic light went into the sample cell. The emitted radiation was detected by the photomultiplier which was at a position perpendicular to the monochromatic light.

The set-up is illustrated in Fig 3.

A black box was used to cover the set-up. The dark current was bucked out by the dark current control of the recorder. The voltage for the photomultiplier was 800 volts. The excitation spectrum of CH_3CHO was recorded from 4000 Å to 3000 Å with a scanning speed 25 Å / min.

Fig. 3 The Apparatus for the Excitation Spectrum of CH_3CHO

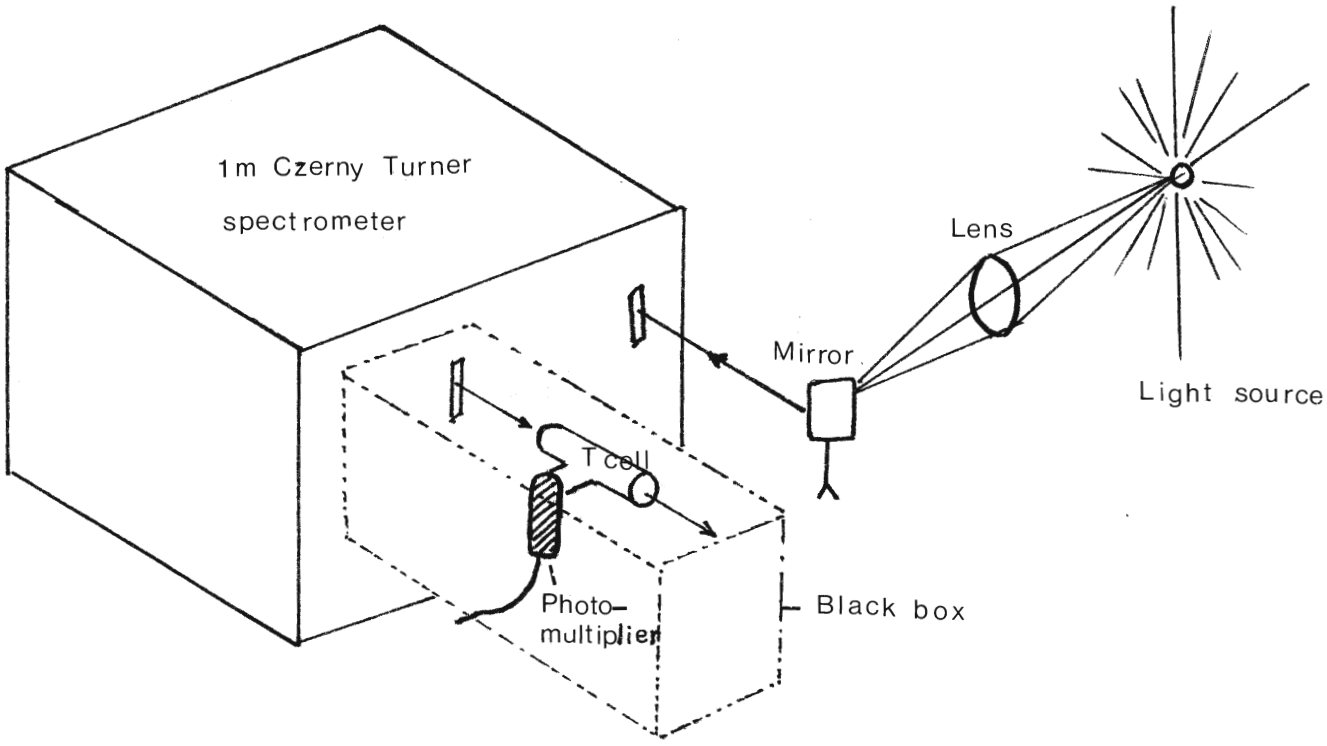
1m Czerny Turner
spectrometer
Lens
Mirror
Light source
T cell
Photo-
multiplier
Black box

(f) Miscellaneous

The 450 watt xenon arc lamp was used as the light source throughout procedure (a), (b), and (c). The spectra in Part (a), (b) and (c) were recorded on the Kodak spectrum analysis SA 1 film. The films were processed in Kodak D-19 developer and Kodak rapid fixer.

The wavenumbers for the spectral lines for all spectra were measured according to the dispersions of the spectra and the distance between the spectral line and the iron wavelength standards. The iron wavelength standards were obtained from the table of Crosswhite[19] and the table from N.R.C.[20].

The optical densities of the spectra in part (a) were measured by a Joyce-Loebl Model III C double beam microdensitometer.

CHAPTER 4

Results

(A) Observed Band Patterns

In the present research, the low resolution absorption spectra recorded with the Baush and Lomb grating spectrograph for the four isotopic compounds of acetaldehyde at room temperature were used to compare with the calculated satellite band patterns which will be described in the following section.

The spectra are shown in Fig. 4 . In these spectra, the point at a wavelength of 3500 Å has been used to divide each spectrum into two zones of transitions. The bands at the longer wavelength ($\lambda > 3500$ Å) zone showed themselves to be much simplier, but less intense structures when compared with the bands in the shorter wavelength ($\lambda <$ 3500 Å) zone (see Fig. 4).

The other spectra obtained in Chapter 3 will be described in the last section of this Chapter.

Fig. 4 The Low Resolution Absorption Spectra for the four Isotopic Compounds of Acetaldehyde at Room Temperature and Low Temperatures.

-50 C
25 C
CH3CHO
27061
27101
27106
27151
27281
27322
27353
27405
27413
27422
27429
27438
27449
27463
27473
27484
27490
27548
27577

25 C
CH3CDO
27397
27466
27484
27597
27618
27652
27669
27736
27760
27783
27893
27903
27932
27976

-50 C
25 C
CD3CHO
27425
27514
27617
27630
27664
27708
27712
27763
27770
27876
27883
27893
27898
27908
27915

-50 C
25 C
CD3CDO
27493
27521
27526
27540
27549
27598
27646
27671
27705
27741
27745
27751
27824
27836
27850
27856

-50 C
25 C
CH_3CHO
27577
27603
27646
27655
27663
27670
27684
27697
27786
27794
27806
27815
27827
27900
27929
27935
27940
27964
27972
28031
28059
28069
28075
28082
25 C
CH_3CDO
27976
28010
28020
28035
28099
28126
28138
28142
28207
28215
28226
28260
28286
28397
28441
28456
-50 C
25 C
CD_3CHO
27915
27980
27988
27990
28004
28014
28033
28082
28098
28105
28111
28115
28176
28192
28195
28352
28362
28387
-50
25
CD_3CDO
27824
27836
27850
27856
27875
27927
27934
27964
27988
27995
28025
28039
28046
28075
28080
28130
28140
28332

CH_3CHO
-50 C
25 C
28082
28111
28148
28163
28173
28192
28204
28305
28422
28442
28524
28538
28572
28585
28609
CH_3CDO
25 C
28397
28441
28456
28483
28508
28534
28651
28700
28710
28730
28742
28798
28839
28845
28888
CD_3CHO
-50 C
25 C
28387
28433
28520
28608
28638
28677
28687
28768
28781
28792
28838
28856
28870
28879
28925
28936
CD_3CDO
-50 C
25 C
28332
28408
28462
28571
28591
28661
28671
28792
28809

-50 C
25 C
CH3CHO
28609
28678
28692
28703
28716
28724
28732
28744
28766
28775
28787
28793
28836
28846
28858
28870
28885
28898
29008
29021
29032
29050
29103
25 C
CH3CDO
28888
28901
28913
28971
28978
28985
29016
29030
29074
29126
29163
29204
29214
29221
29228
29328
29336
-50 C
25 C
CD3CHO
28936
28990
29001
29008
29018
29034
29044
29086
29099
29103
29120
29128
29135
29154
29162
29179
29237
29296
29323
29357
29385
29403
29433
29441
29474
29495
29508
-50
25
CD3CDO
28809
28898
28943
28962
28968
28992
29006
29033
29044
29075
29102
29145
29151
29174
29189
29195
29202
29248
29282
29312
29342
29371
29375
29415

-65 c
25 c
CH3CHO
29021
29050
29103
29190
29204
29211
29335
29346
29337
29415
29449
29530
25 c
CH3CDO
29336
29353
29388
29398
29475
29561
29597
29623
29645
29689
29697
29704
29711
29734
29748
29793
29800
29838
29886
-65 c
25 c
CD3CHO
29508
29569
29575
29651
29681
29701
29715
29808
29818
29846
29942
29949
30067
30075
-65 c
25 c
CD3CDO
29415
29452
29462
29473
29511
29522
29534
29607
29618
29661
29668
29748
29761
29789
29996
29837
29849
29855
29879
29886
29936
29955
29973
29983
29991

-75 C
25 C
CH_3CHO
29530
29541
29563
29671
29703
29717
29770
29779
29799
29824
29827
29843
29850
29878
29988
30008
30042
30054
25 C
CH_3CDO
29886
29935
29956
29981
29995
30014
30022
30040
30069
30081
30131
30148
30178
30243
30271
30307
30367
-75 C
25 C
CD_3CHO
30075
30174
30179
30189
30261
30278
30298
30303
30364
30402
-75 C
25 C
CD_3CDO
29991
30033
30081
30090
30143
30183
30206
30212
30295
30319
30382
30419
30433
30545
30550

The values of barrier heights, V_3' , and the internal rotation constants, F' for the excited state were set arbitrarily in the trial calculations. The range of V_3' was chosen to be between 200 cm^{-1} and 600 cm^{-1}, and the value of F' was assumed to be equal to the ground state value. If both ground state and excited state constants of V_3 and F are known, the torsional satellite band pattern for the isotopic compounds of acetaldehyde can then be obtained from the computer program mentioned in Chapter 1 .

The output of this computer program generated two kinds of satellite band patterns. The first one was the barriers-in-phase case which corresponded to two H-H staggered conformations of acetaldehyde in both electronic states. The second one was the barriers-out-of-phase case which corresponded to a H-H elcipsed conformation in the excited state and a H-H staggered conformation in the ground state. (see Fig. 5)

The potential curves and the calculated satellite band patterns for CH_3CHO in the in-phase case and the out-of-phase case are illustrated in Figs.7 and 6 respectively. In Figs. 6 and 7 the torsional angle Ø of 0 ,120,240 deg corresponded to a H-H elcipsed conformation while the Ø of 60,180, 300 deg corresponded to a H-H staggered conformation.

In the ground state the structural parameters of CH_3CDO were assumed to the same as CH_3CHO and the barrier height for CH_3CDO was assumed to be 400 cm^{-1} .

The ground state moments of inertia and the internal rotation constants, F , for the four isotopic compounds of acetaldehyde were then calculated from their ground state structural parameters according to equation (5) and (7) in Chapter 2. The values are listed in Table 4.

Table 4

Moments of inertia (I_a , I_b , I_c) and internal rotation constants (F'') for four isotopic compounds of acetaldehyde

Compound	I_a	I_b	I_c	F''
		(amu A^2)		(cm^{-1})
CH_3CHO	8.933	49.741	55.553	7.679
CH_3CDO	10.599	50.346	57.823	7.056
CD_3CHO	12.114	58.853	64.672	4.988
CD_3CDO	14.456	58.936	55.553	4.440

(B) Calculated Band Patterns

The ground state structures of the isotopic compounds of acetaldehyde have been studied by Kilb, Lin and Wilson[10]. The ground state structural parameters and the barriers to internal rotation for CH_3CHO, CD_3CHO and CD_3CDO obtained by these workers are listed in Table 3, with r and θ representing the bond length and the bond angle respectively.

Table 3

Structural Parameters and Barrier Heights for Isotopic Compounds of Acetaldehyde

---

Structural parameters

r (c-c) = 1.5005 Å

r (c=o) = 1.2155 Å

θ (c-c=o) = 123° 55′

Methyl r (c-H) = 1.086 Å , θ (HCH) = 108° 16′

r (c-D) = 1.088 Å , θ (DCD) = 108° 32′

Aldehyde r (c-H) = 1.114 Å, θ (c-c-H) = 117° 29′

r (c-D) = r (c-H) assumed

θ (c-c-H) = θ (c-c-D) assumed

Barrier heights

V_3 (CH_3CHO) = 406.42 cm^{-1}

V_3 (CD_3CHO) = 402.57 cm^{-1}

V_3 (CD_3CDO) = 399.77 cm^{-1}

Fig. 5 The Conformations in the excited states illustrating the barriers-in-phase case and the barriers-out-of-phase case

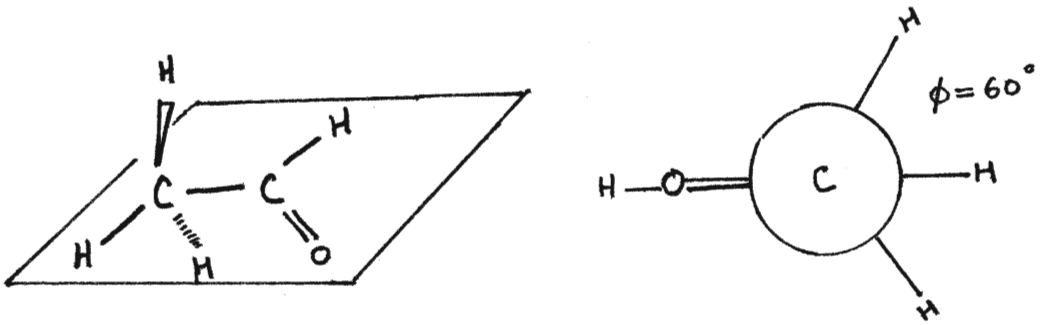

Barriers-in-phase Case

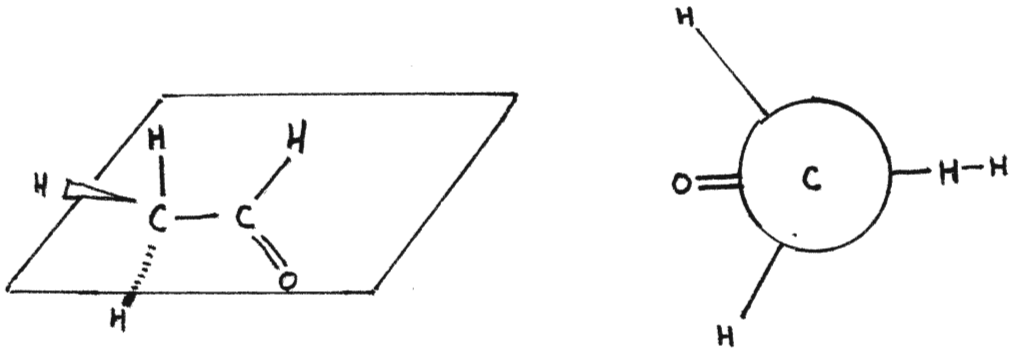

Barriers-out-of-phase Case

Fig. 6 Potential Curves, Energy Levels, Principal Transitions and Calculated Satellite Band Structure for Torsional Electronic Transition of CH_3CHO- Barriers-in-phase case : $V_3' = 511\ cm^{-1}$, $F' = 8.089\ cm^{-1}$

$V_3'' = 406.42\ cm^{-1}$, $F'' = 7.679\ cm^{-1}$

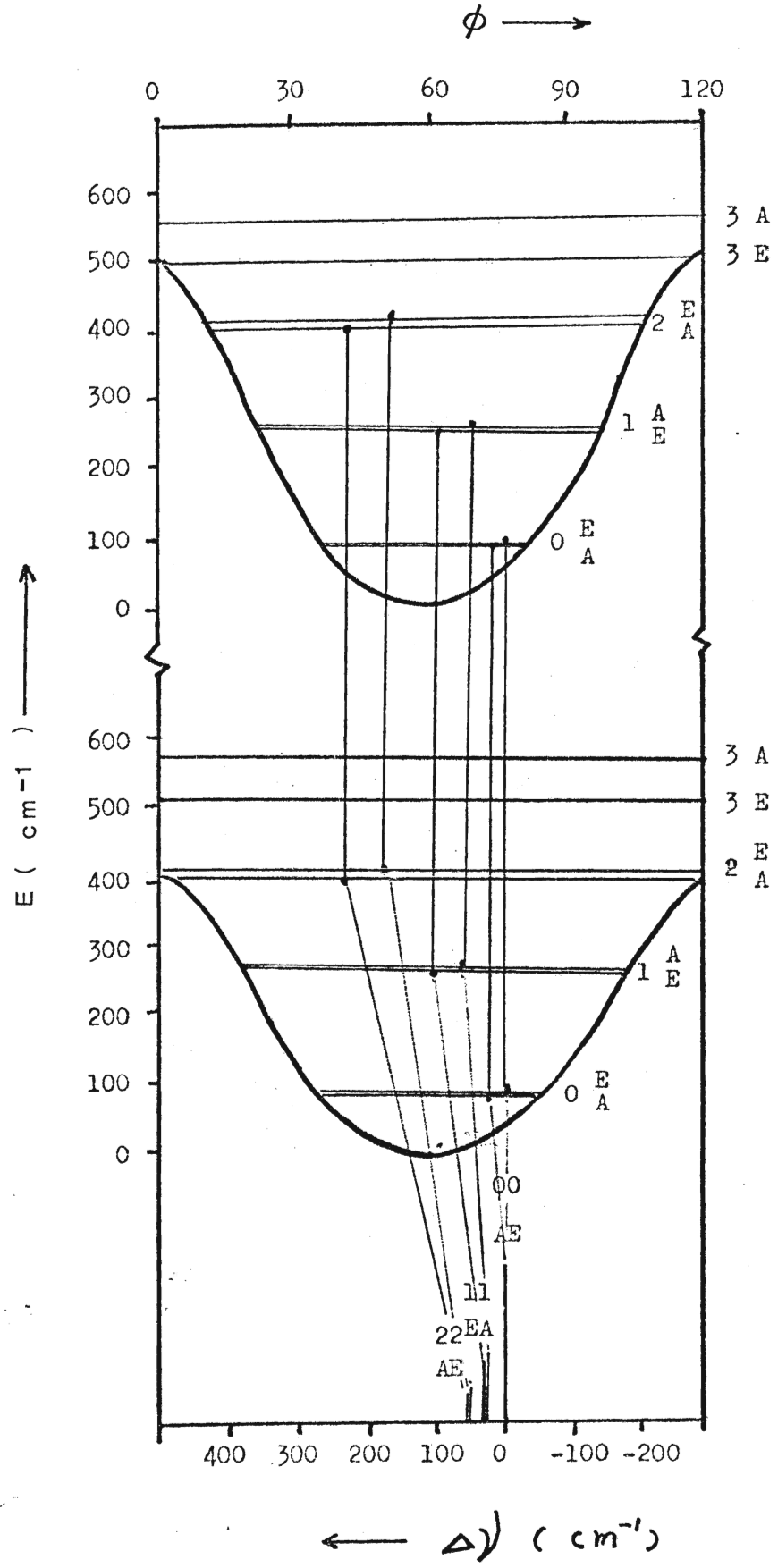
φ
0
30
60
90
120
600
500
400
300
200
100
0
3 A
3 E
2 E
A
1 A
E
0 E
A
E (cm-1)
00
AE
11
22 EA
AE
400
300
200
100
0
-100
-200
Δν (cm-1)

Fig. 7 Potential Curves, Energy Levels, Principal Transitions and Calculated Satellite Band Structure for Torsional Electronic Transition of CH_3CHO - Barriers-out-of-phase case : $V_3' = 511\ cm^{-1}$, $F' = 8.089\ cm^{-1}$

$V_3'' = 406.42\ cm^{-1}$, $F'' = 7.679\ cm^{-1}$

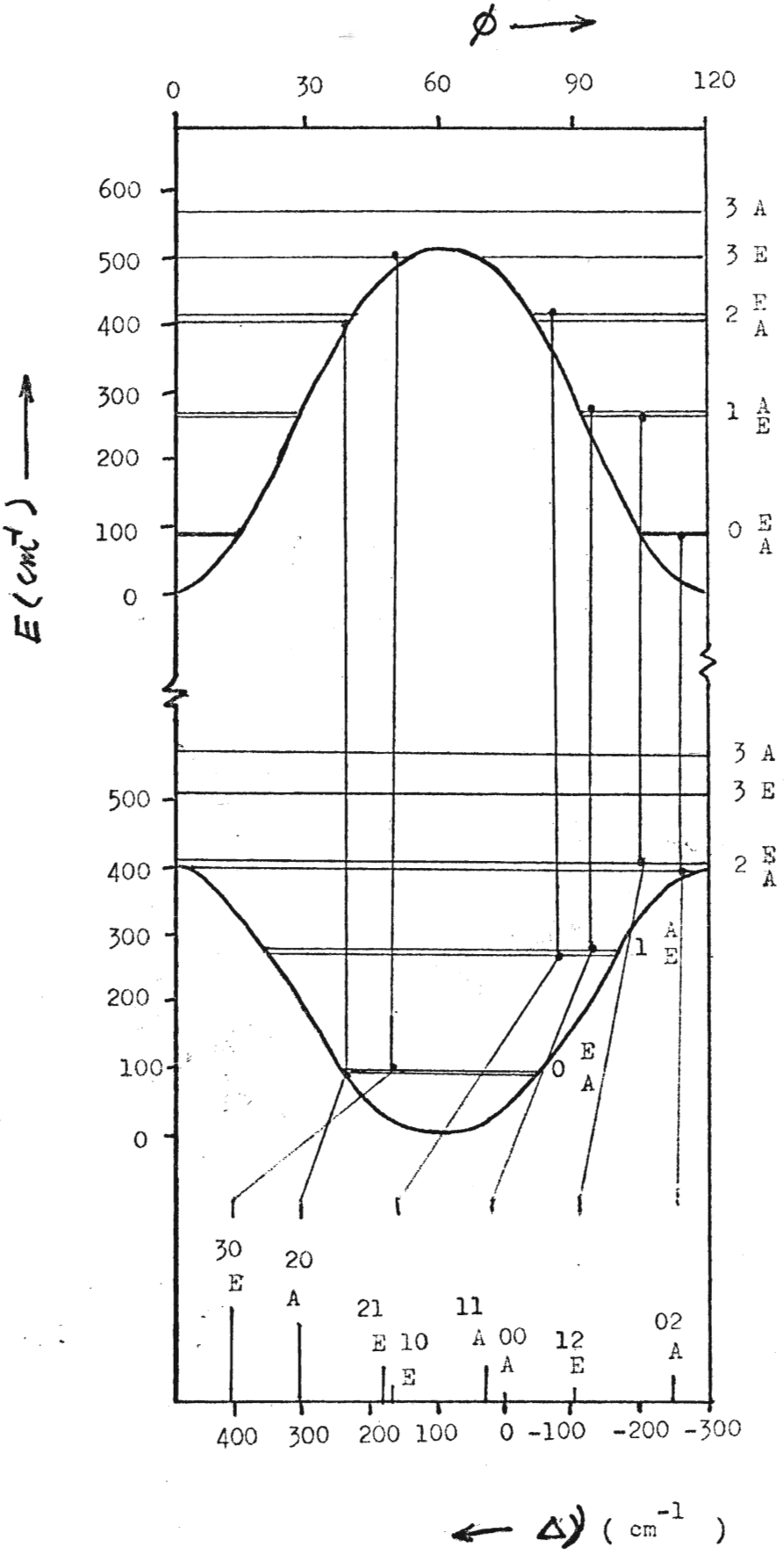
φ →
0
30
60
90
120
E (cm⁻¹) →
600
500
400
300
200
100
0
3 A
3 E
2 E
A
1 A
E
0 E
A
3 A
3 E
2 E
A
1 A
E
0 E
A
30
E
20
A
21
E
10
E
11
A
00
A
12
E
02
A
400
300
200
100
0
-100
-200
-300
← Δν (cm⁻¹)

When the barrier height in the excited state was changed from 200 cm^{-1} to 600 cm^{-1} , the patterns with different energy spacings were produced. An example for CH_3CHO in the barriers-in-phase case is illustrated in Fig. 8 and an example for CH_3CHO in the barriers-out-of-phase case is illustrated in Fig. 9 .

In the patterns for the barriers-in-phase case , the strongest band was the 0-0 band and the intensities of the other bands decreased rapidly. In the patterns for the barriers-out-of-phase case, the 0-0 band was weak and the intensities of the other bands did not decrease rapidly, so that more transitions were active in the spectrum.

The notation ($v'_a v''$) was used to label the transition. For example , $^4A^0$ represented a transition from a ground state , v=0 , A level to an excited state , v = 4 , A level.

Fig. 8 The Calculated Satellite Band Structure for the Electronic Transitions involving the Torsional Mode of CH_3CHO - Barriers-in-phase case : $V_3'' = 406.42\ cm^{-1}$, $F'' = F' = 7.679\ cm^{-1}$

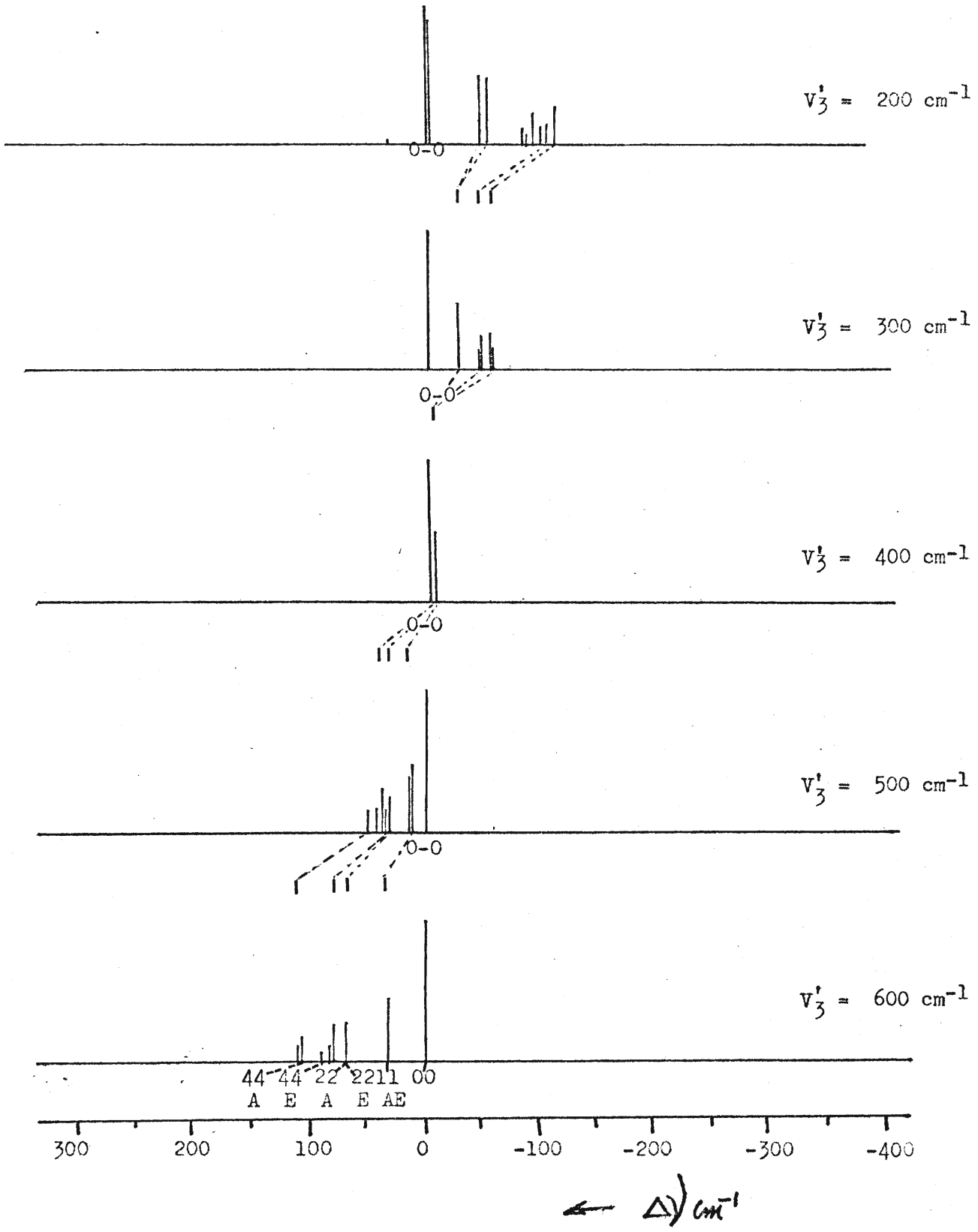
V_3' = 200 cm^{-1}
0-0
V_3' = 300 cm^{-1}
0-0
V_3' = 400 cm^{-1}
0-0
V_3' = 500 cm^{-1}
0-0
V_3' = 600 cm^{-1}
44 44 22 2211 00
A E A E AE
300
200
100
0
-100
-200
-300
-400
← Δν cm^{-1}

Fig. 9 The Calculated Satellite Band Structure for the Electronic Transitions involving the Torsional Mode of CH_3CHO - Barriers-out-of-phase case : $v'' = 406.42\ cm^{-1}$, $F'' = F' = 7.679\ cm^{-1}$

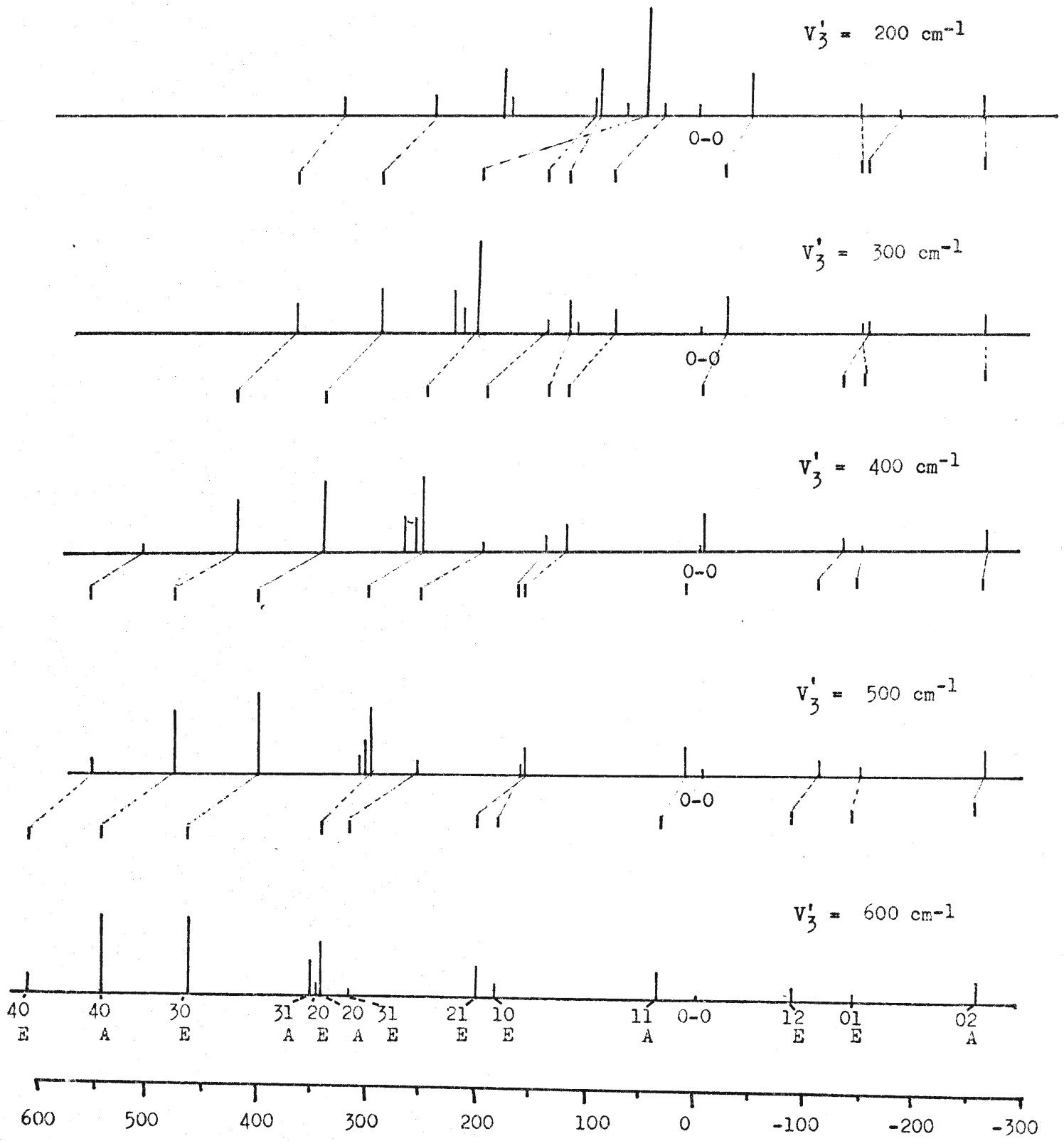
V_3' = 200 cm^{-1}
0-0
V_3' = 300 cm^{-1}
0-0
V_3' = 400 cm^{-1}
0-0
V_3' = 500 cm^{-1}
0-0
V_3' = 600 cm^{-1}
40 E
40 A
30 E
31 A
20 E
20 A
31 E
21 E
10 E
11 A
0-0
12 E
01 E
02 A
600
500
400
300
200
100
0
-100
-200
-300
← Δν (cm^{-1})

(C) Comparison between the Calculated and Observed Band Pattern

Each of the two calculated patterns ,i.e. one for the barriers-in-phase case and one for the barriers-out-of-phase case was compared to the bands in both zones in the observed spectrum.

The bands in the longer wavelength ($\lambda > 3500$ Å) zone were selected to compare with the calculated satellite band patterns. The patterns for the barriers-in-phase case and for the barriers-out-of-phase case were used respectively.

In the barriers-in-phase case, two things were found when the strongest band in the longer wavelength zone was assigned to be the O-O band in the calculated pattern : firstly, the energy spacings among the observed bands were different from the calculated spacings and secondly, the intensities of the observed bands did not decrease rapidly as shown in Fig. 8 . Therefore , the assumption that for the two barriers should be in phase with respect to each other was rejected.

The observed spectrum was than compared with the patterns for the barriers-out-of-phase case. Here, the observed satellite band structures were found to be more similar to the calculated band structures than in the barriers-in-phase case.

The excited state barrier heights in the selected calculated pattern were close to 500 cm^{-1}.

The comparison between the trace of optical densities and the calculated band patterns for the four isotopic compounds of acetaldehyde are shown in Fig. 10 .

Fig. 10 The Comparison between the Densitometer Trace of the Absorption Spectra and the Calculated Band Satellite Patterns of the four Isotopic Compounds of Acetaldehyde : A) CH_3CHO , B) CH_3CDO , C) CD_3CHO, D) CD_3CDO

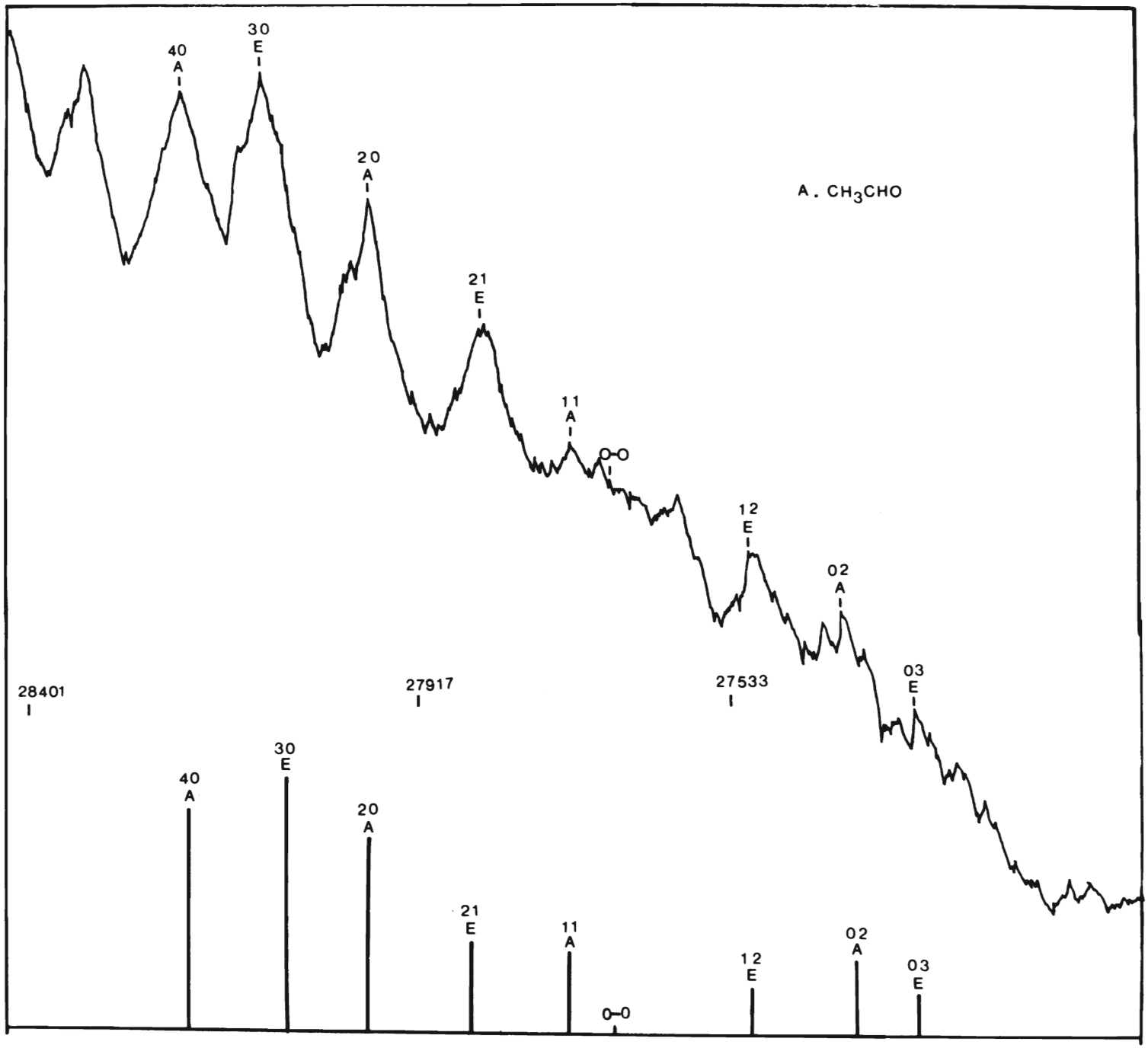
40 A
30 E
20 A
21 E
11 A
0–0
12 E
02 A
03 E
A. CH_3CHO
28401
27917
27533
40 A
30 E
20 A
21 E
11 A
0–0
12 E
02 A
03 E

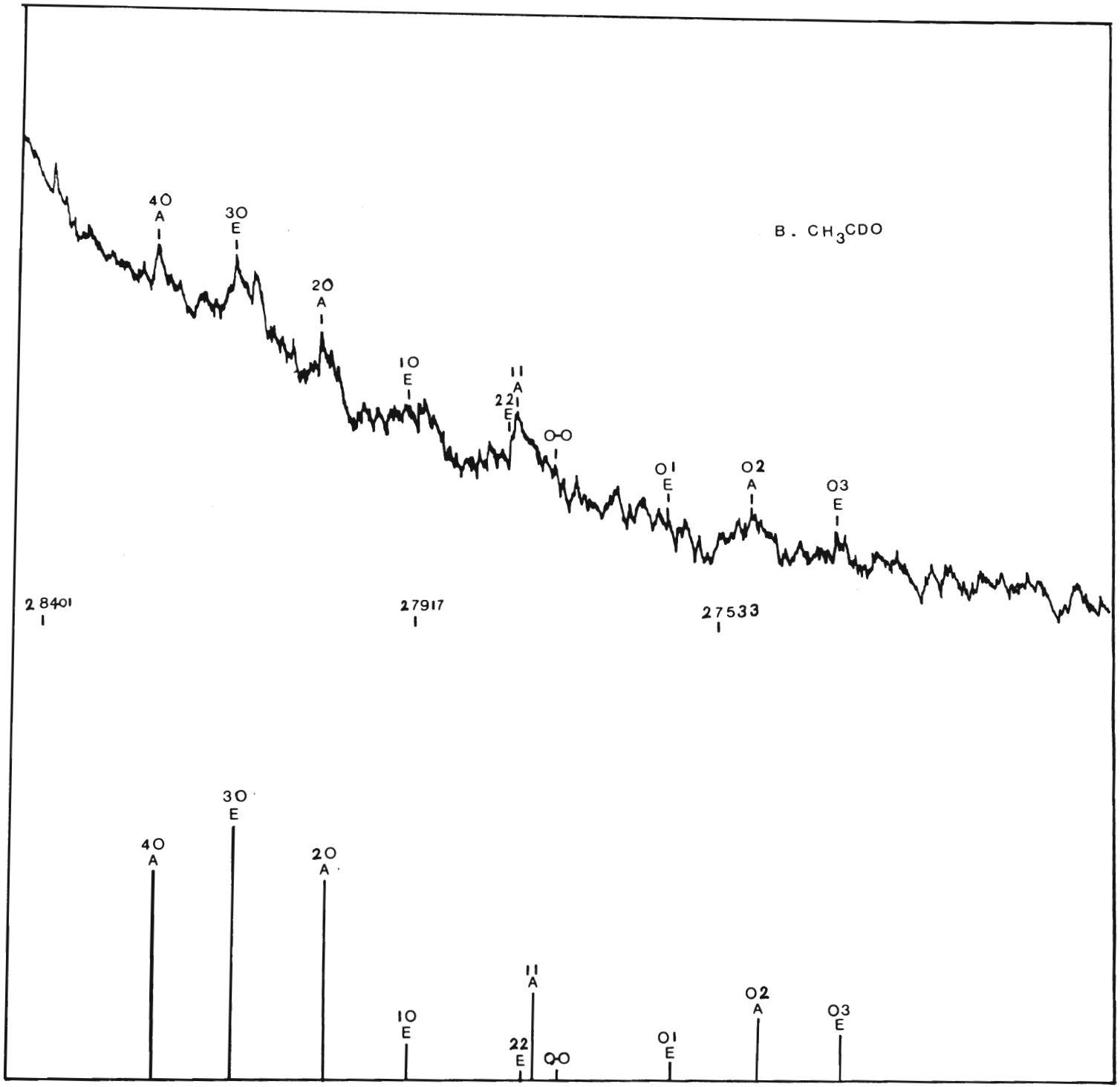
B. CH_3CDO
40 A
30 E
20 A
10 E
11 A
22 E
O-O
01 E
02 A
03 E
2.8401
2.7917
2.7533

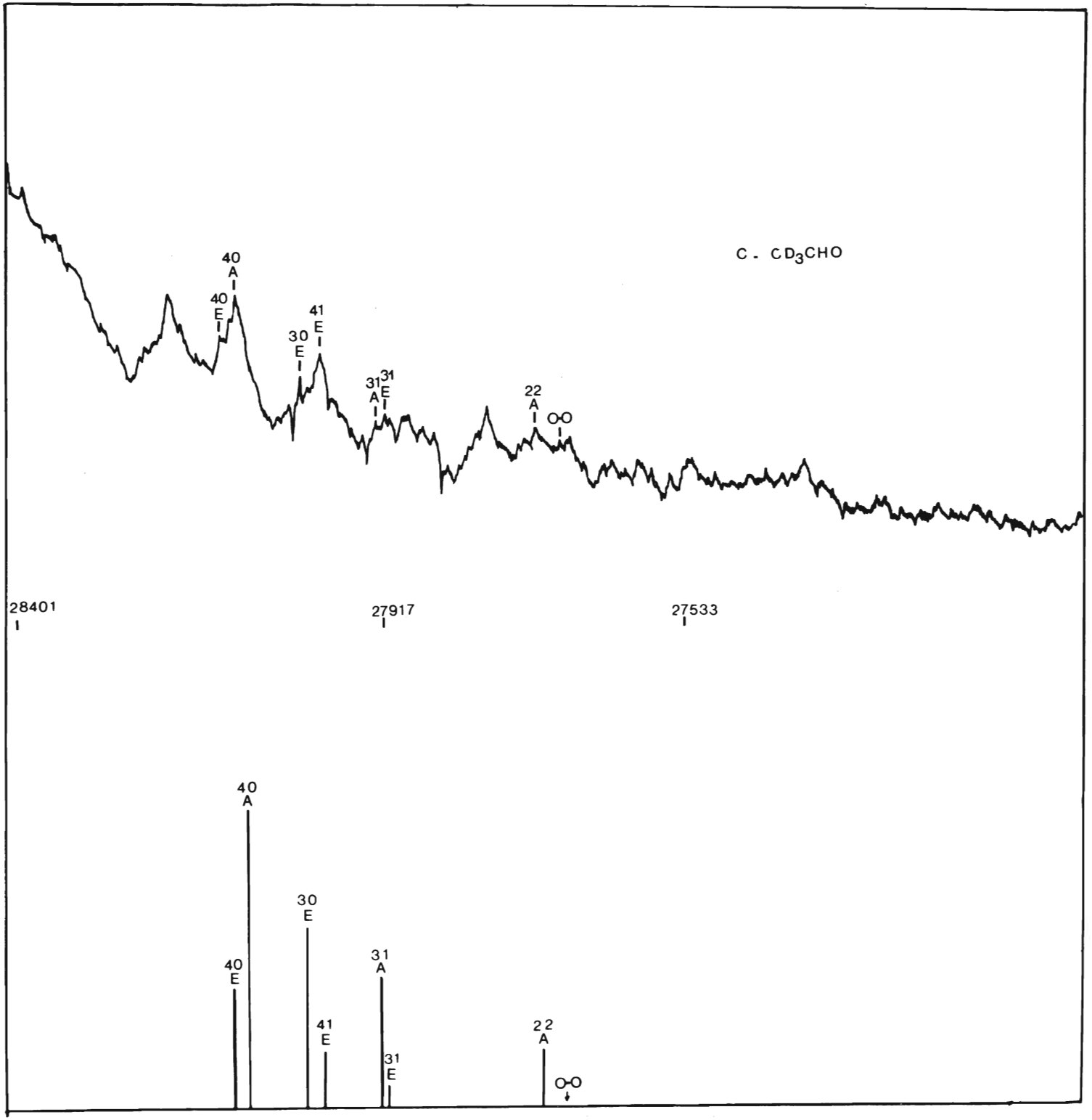
C - CD_3CHO
40 A
40 E
30 E
41 E
31 A
31 E
22 A
O-O
28401
27917
27533
40 A
40 E
30 E
41 E
31 A
31 E
22 A
O-O

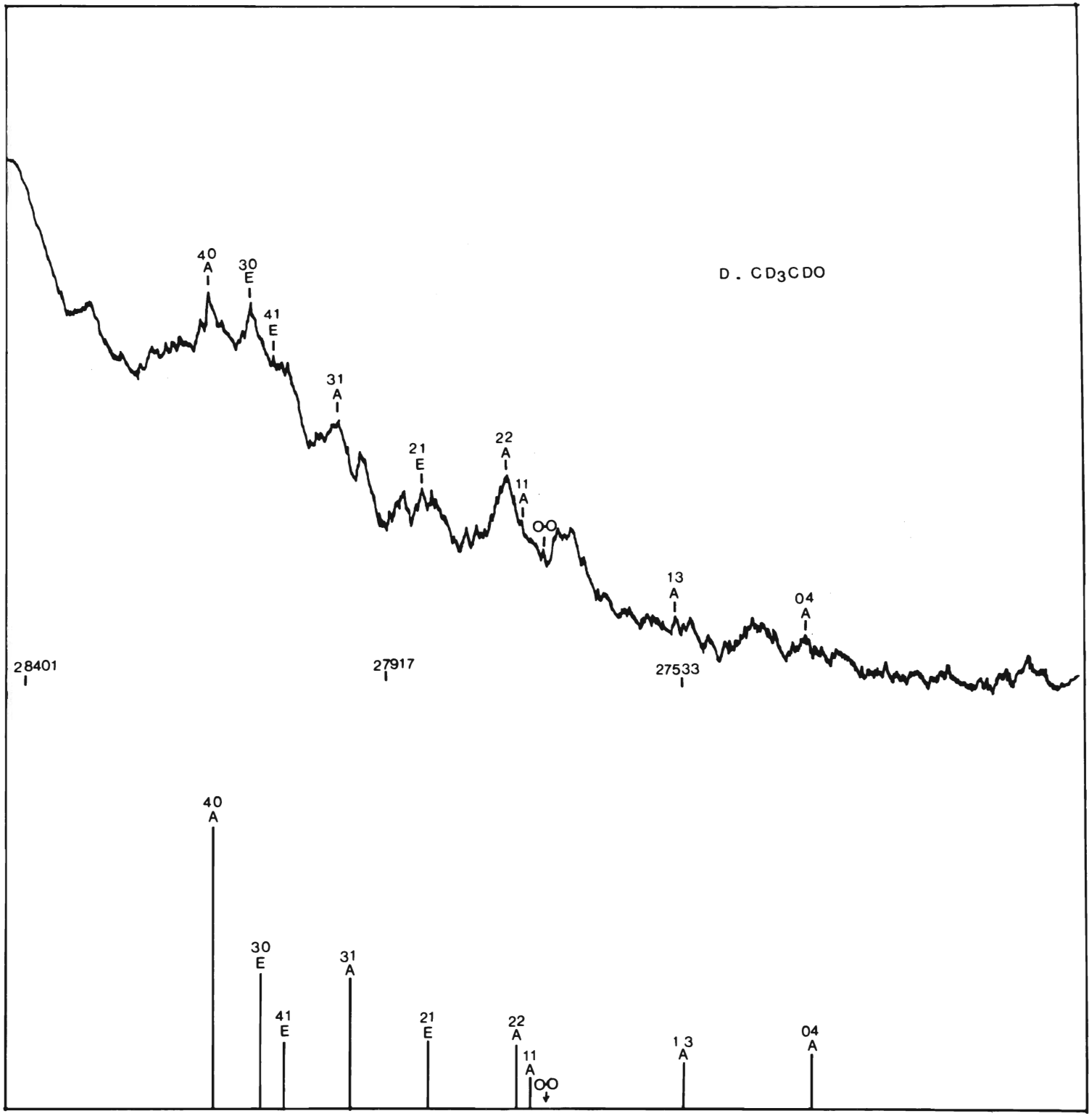
D . CD3CDO
40 A
30 E
41 E
31 A
21 E
22 A
11 A
OO
13 A
04 A
28401
27917
27533
40 A
30 E
41 E
31 A
21 E
22 A
11 A
OO
13 A
04 A

A least squares programme was used to obtain a reasonable fit for the transition energies. The input data included the barrier heights, the internal rotation constants for both ground and excited states and the frequency of the O-O band. After a few rounds of calculations, a satifactory fit for the observed and calculated transitions was generated as well as the new values for the barrier height, the internal rotation constant and the frequency of the O-O band.

The assigned transitions involving the torsional mode of the isotopic compounds of acetaldehyde are shown in Tables 5, 6, 7 and 8.

Table 5

The Observed and the Calculated Electronic Transitions involving the Torsional Mode of CH_3CHO from the Least Squares Analysis

v'	v''	∝	observed frequency	precision (cm^{-1})	calculated frequency	residue
4	0	A	28173	2.0	28171.6	1.4
3	0	E	28082	2.0	28082.2	-0.2
2	0	A	27973	3.0	27974.8	-1.8
1	1	A	27697	2.0	27697.5	-0.5
0	2	A	27413	2.0	27413.7	-0.7
0	3	E	27322	2.0	27321.5	0.5
1	2	E	27573	3.0	27569.7	3.3
3	1	A	28007	2.0	28006.8	0.2
2	1	E	27845	2.0	27845.5	-0.5

Table 6

The Observed and the Calculated Electronic Transitions involving the Torsional Mode of CH_3CDO in the least Squares Analysis

v'	v''	↶	observed frequency	precision (cm^{-1})	calculated frequency	residue
4	0	A	28215	2.0	28215.3	-0.3
2	0	A	28035	2.0	28034.9	0.1
1	0	E	27903	2.0	27901.3	1.7
1	1	A	27760	2.0	27760.2	-0.2
2	2	E	27783	2.0	27782.3	0.7
0	1	E	27597	2.0	27595.8	1.2
0	2	A	27484	2.0	27485.6	-1.6
3	0	E	28138	2.0	28138.1	-0.1
0	3	E	27397	2.0	27398.0	-1.0

Table 7

The Observed and the Calculated Electronic Transitions involving the Torsional Mode of CD_3CHO in the Least Squares Analysis

v'	v''		observed frequency	precision (cm^{-1})	calculated frequency	residue
2	2	A	27710	2.0	27708.3	1.7
3	1	E	27908	2.0	27909.9	-1.9
3	1	A	27916	2.0	27918.4	-2.4
3	0	E	28033	2.0	28031.3	1.7
4	0	A	28096	2.0	28096.3	-0.3
4	1	E	28004	3.0	28001.0	3.0
4	0	E	28125	3.0	28122.4	2.6
4	2	E	27893	2.0	27893.3	-0.3

Table 8

The Observed and Calculated Electronic Transitions involving the Torsional Mode of CD_3CDO in the Least Squares Analysis

v'	v''	σ	observed frequency	precision (cm^{-1})	calculated frequency	residue
2	1	E	27856	2.0	27856.0	0.0
1	1	A	27741	2.0	27740.4	0.6
3	1	A	27961	2.0	27960.0	1.0
0	4	A	27379	2.0	27377.3	1.7
1	3	A	27540	2.0	27542.1	-2.1
4	0	A	28140	2.0	28140.5	-0.5
3	0	E	28075	3.0	28070.7	4.3
4	1	E	28046	2.0	28044.8	1.2
2	2	A	27752	2.0	27754.0	-2.0

The new O-O band frequencies, the barrier heights and the internal rotation constants for the four isotopic compounds of acetaldehyde calculated by the least squares procedure are listed in Table 9.

Table 9

The Refined Constants (V' , F' , ν_{0-0}) for the four Isotopic Compounds of Acetaldehyde (in cm^{-1})

Compound	V'	F'	ν_{0-0}
CH_3CHO	472.65	8.945	27673.1
CH_3CDO	490.35	7.747	27736.5
CD_3CHO	484.05	4.482	27689.8
CD_3CDO	502.02	4.158	27729.3

(D) Miscellaneous Findings

The long path length (91.43 m) and low resolution absorption spectrum of CH_3CHO is illustrated in Fig. 11. In Fig. 11 , some of the weak bands with wavelengths longer than 3664 Å were observed. Under the conditions of high pressure and long path length, the singlet-triplet transition of acetaldehyde is expected to be observed.

Portions of the first order high resolution spectra for the four isotopic compounds of acetaldehyde are illustrated in Fig. 12. The position of the 0-0 bands are indicated by the arrows in Fig. 12 .

A part of the 17 th order high resolution spectrum of CH_3CHO is illustrated in Fig. 13 . It showed that the bands near 3500 Å were diffuse and weak, and the position of 0-0 band could not be recorded.

The fluorescence and the excitation spectra of CH_3CHO are shown in Fig. 14 . The intercept of these two curves indicated the 0-0 band to be at 3620 Å (27624 cm^{-1}).

Fig. 11 The Long Path Length and Low Resolution Absorption Spectrum of CH_3CHO

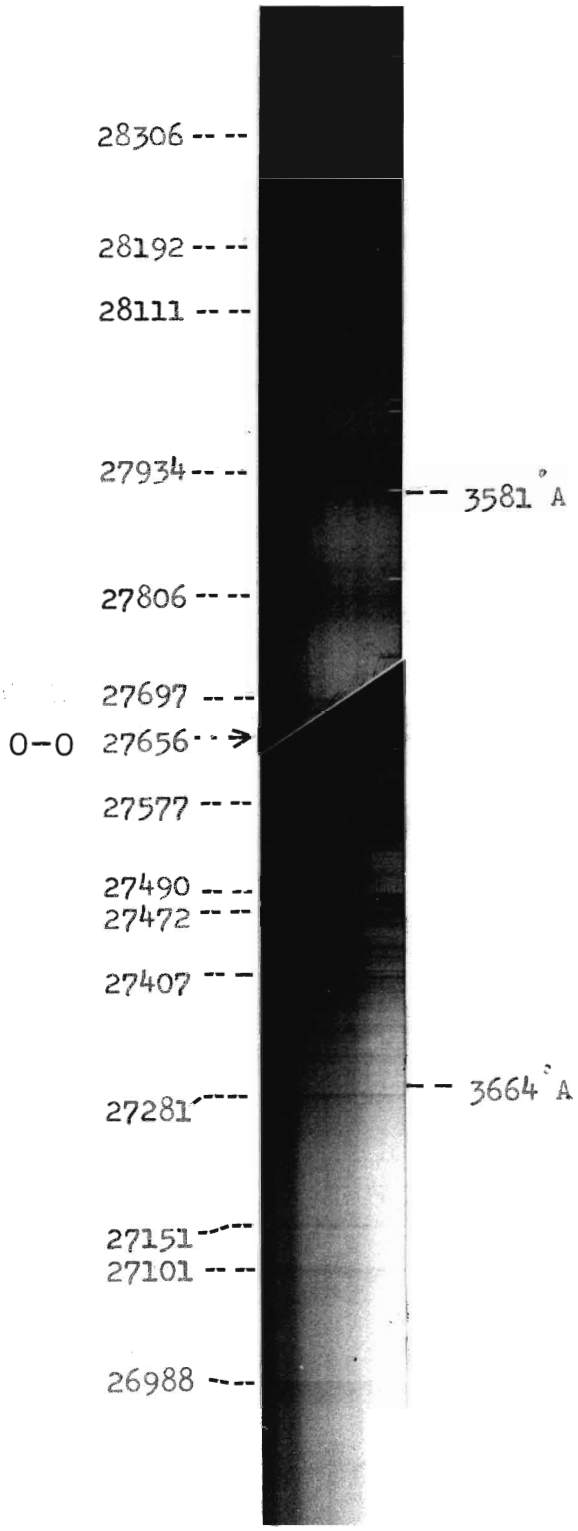
28306
28192
28111
27934
3581 °A
27806
27697
0-0
27656
27577
27490
27472
27407
27281
3664 °A
27151
27101
26988

Fig. 12 Portions of the First Order High Resolution Absorption Spectra of four Isotopic Compounds of Acetaldehyde

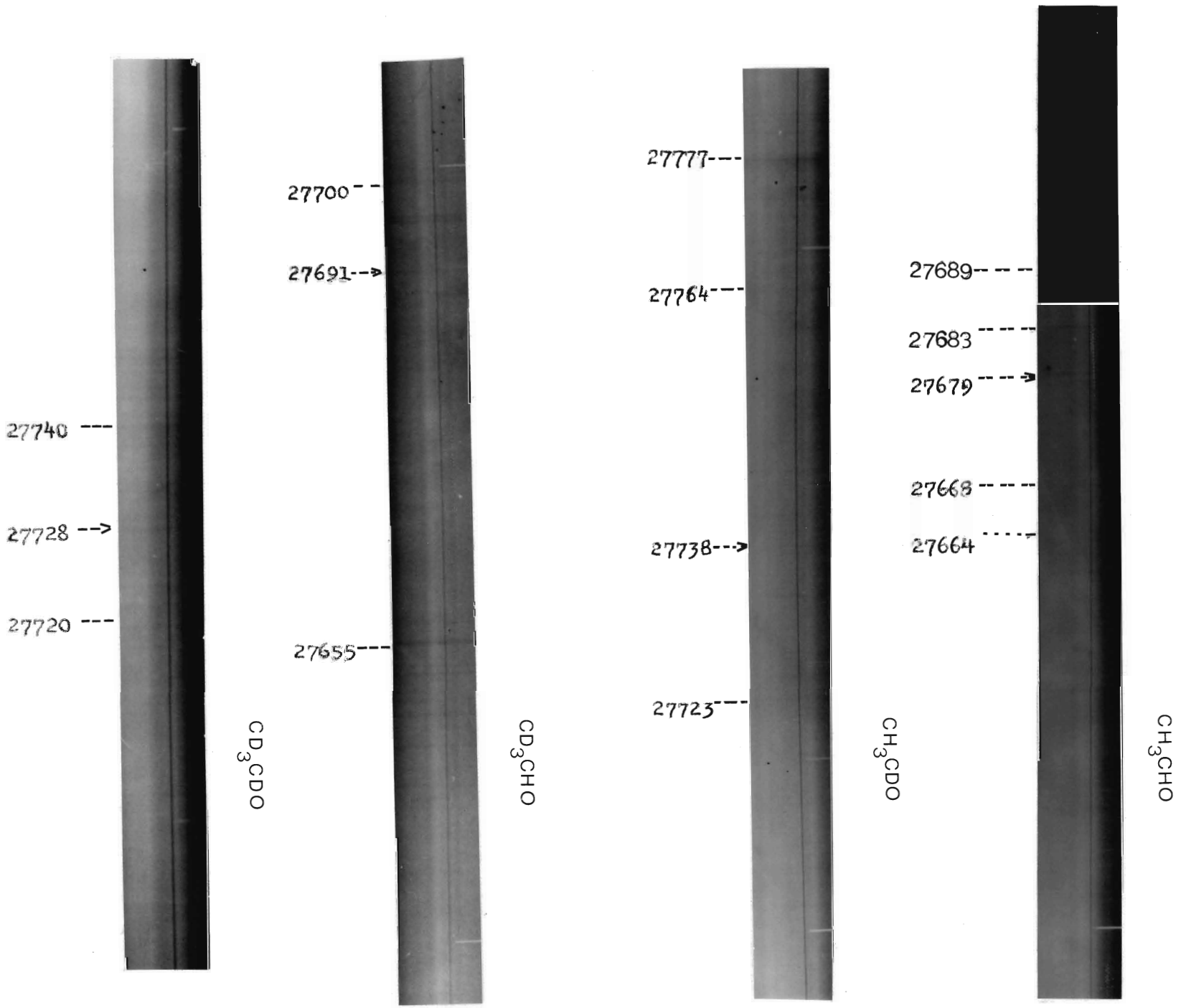
27740
27728
27720
CD_3CDO
27700
27691
27655
CD_3CHO
27777
27764
27738
27723
CH_3CDO
27689
27683
27679
27668
27664
CH_3CHO

Fig. 13 The 17 th Order High Resolution Absorption Spectrum of CH_3CHO

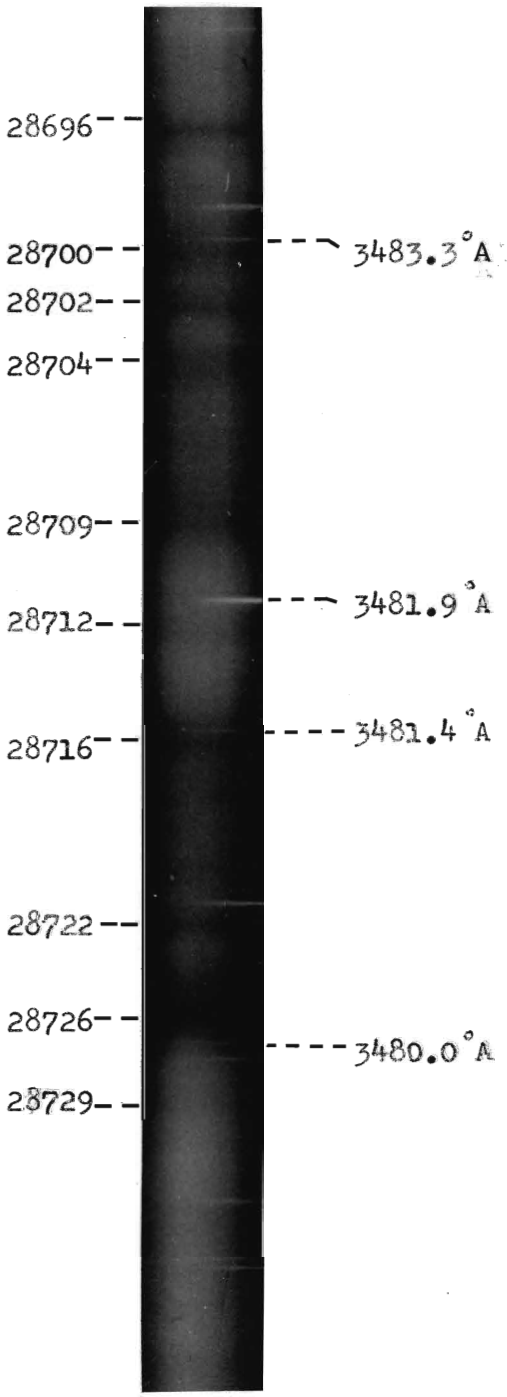
28696
28700
28702
28704
28709
28712
28716
28722
28726
28729
3483.3°A
3481.9°A
3481.4°A
3480.0°A

Fig. 14 The Fluorescence and the Excitation Spectra of CH_3CHO

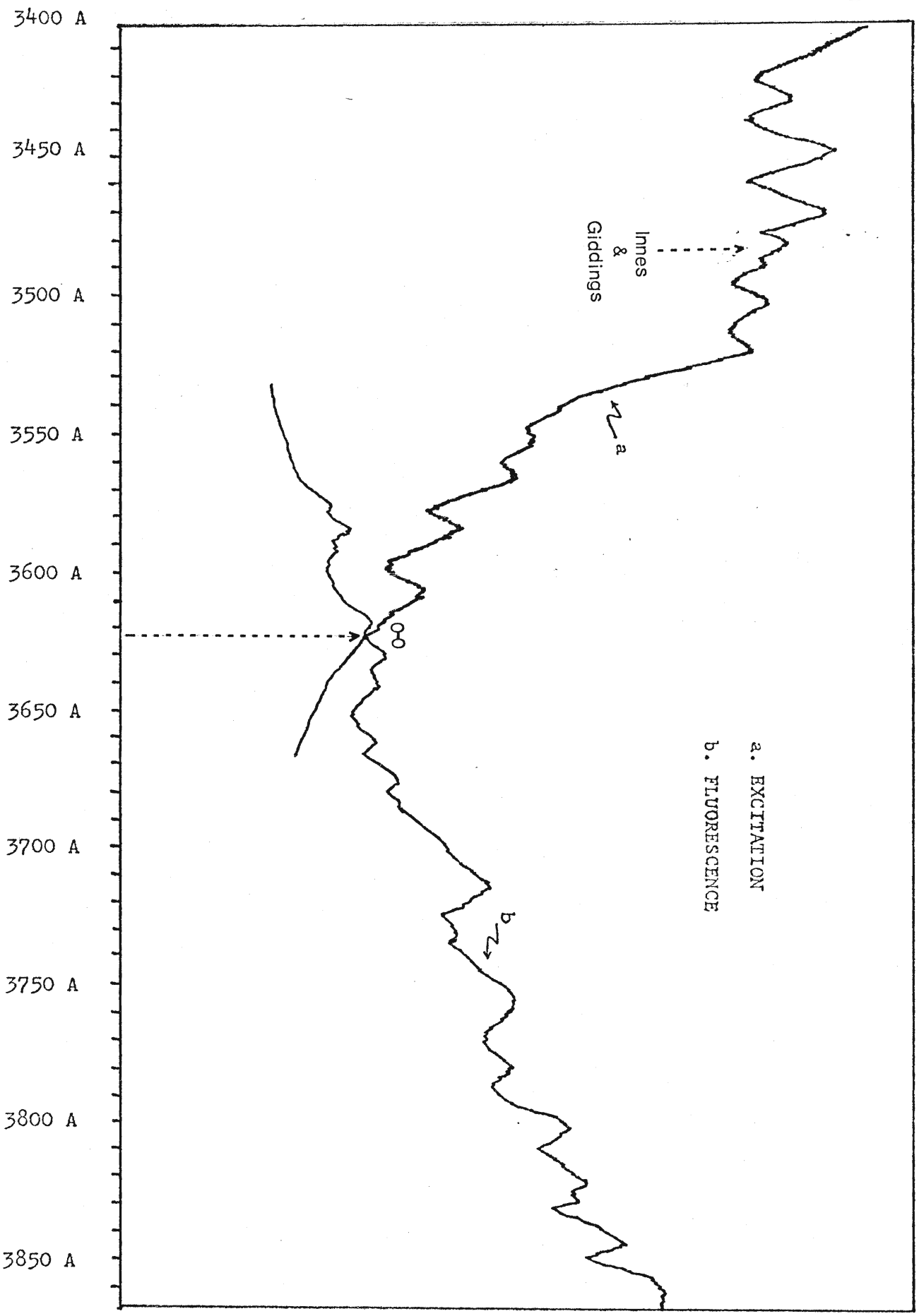
INTENSITY
3400 A
3450 A
3500 A
3550 A
3600 A
3650 A
3700 A
3750 A
3800 A
3850 A
Innes
&
Giddings
a
b
00
a. EXCITATION
b. FLUORESCENCE

CHAPTER 5

Discussion

At the initial stage of the calculation, the barrier height of acetaldehyde in the excited state was unknown, so that it was necessary to make some predictions about the magnitude of the barrier before using the value to obtain the satellite band pattern. The methods based on the approximate molecular orbital theory were used to compute the barrier height. The computer programs based on these theories were MINDO 3 and INDO.[28] In these methods of calculation, the structural parameters of the molecule were required to remain the same in both conformations, except for the torsional angle. In the MINDO 3 program, the structural parameters of the molecule for each conformation were optimized and therefore the computed barrier height was different from the experimental barrier height. In the INDO program, the Cartesian coordinates of each atom of the molecule were used instead of the structural parameters. In the case of acetaldehyde, the barrier height of the ground state was found to be 406 cm^{-1} and this value was compared with the computed values from the above two computer programs.

By using MINDO 3, five parameters of acetaldehyde were optimized, except for the C-H bond lengths and the H-C-H bond angles of the methyl group. The two torsional angles, 0° and 60° respectively, represented the two conformations in the

ground state and the computed energy difference between these two conformations was 110.29 cm^{-1} . The coordinates of the atoms corresponding to the ground state structure of acetaldehyde were used as the input for the INDO programme and the calculated energy difference between the two conformations was 220.98 cm^{-1}. It was found that both MINDO 3 and INDO could generate lower values of barrier height than the experimental value and the most stable conformation in ground state was the one with one methyl hydrogen eclipsing the C=O bond. When the excited state, i.e. the triplet state, was considered, the calculated barrier height by using MINDO 3 was 69.23 cm^{-1} and the value from INDO was 77 cm^{-1}. The values obtained by these two programmes are listed in Table 10.

Table 10

The Calculated Energy Difference for two Conformations of CH_3CHO using MINDO 3 and INDO

	Ground State	
Conformation	H-H eclipsed	H-O eclipsed
Torsional Angle	$\phi = 0^\circ$	$\phi = 60^\circ$
Total Energy MINDO 3	-624.2993 e.v.*	-624.3130 e.v.
Total Energy INDO	- 34.1908 a.u.**	- 34.1918 a.u.
	Calculated Energy Difference	
MINDO 3	+ 110.29 cm^{-1}	
INDO	+ 220.98 cm^{-1}	
Experimental	+ 406.42 cm^{-1}	
	Excited State	
Total Energy MINDO 3	-621.2725 e.v.	-621.2639 e.v.
Total Energy INDO	- 34.0766 a.u.	- 34.0769 a.u.
	Calculated Energy Difference	
MINDO 3	- 69.23 cm^{-1}	
INDO	+ 77.62 cm^{-1}	

* 1 e.v. = 8050.25 cm^{-1}

** 1 a.u. = 2.19066×10^5 cm^{-1}

In Table 10 , the most stable conformation in the excited state was the H-H eclipsed conformation according to the MINDO 3 calculation, but from the INDO calculation the most stable conformation was H-O eclipsed conformation. The MINDO 3 and INDO ground state values had the factor of ¼ and ½ of the ground state experimental value respectively, so that the predicted excited state values were 280 cm for MINDO 3 and 154 cm for INDO. Because the results from these two calculations were contradictory to each other and the ground state calculated values were too low when compared with the experimental values, none of the predicted values were reliable for the satellite band pattern calculation. Therefore, in this research the only way to compare the observed band patterns with the calculated band patterns was to set the barrier height in the excited state arbitrarity.

The comparisons between the observed and the calculated band patterns of the four isotopic compounds of acetaldehyde showed that the patterns from the barrier-out-of-phase case were active in the absorption spectra. Surprisingly, the patterns generated by the barriers-in-phase cases could not be found in the observed spectra, however, it should appear in the spectra according to the MINDO 3 and INDO predictions due to the potential curves changing the phases in the excited state. It was assumed that the conformational H-H staggered

isomer might have a much higher energy than the H-H eclipsed isomer in the excited state, therefore, the only band pattern was found to be the one in the barriers-out-of-phase case.

The barrier heights for the four isotopic compounds of acetaldehyde were expected to have nearly equal values in the excited state, because their ground state values had only $\pm$ 10 % difference. This assumption could be confirmed by the fact that the refined values of excited state barriers of the four isotopic compounds were close to 500 cm^{-1} . The refined values for the internal rotation constants were changed $\pm$ 10 % of their ground state values. This showed that the geometrical structures of the compounds in their excited states were different from those in the ground states. The changes of the structures could be possibly due to the lengthening of C=O bond and C-C bond , or the aldehyde hydrogen moving out of the symmetry plane. For example, if the aldehyde hydrogen was out of the plane with a small angle,i.e. 5° , the internal rotation constant of CH_3CHO would change from 7.679 cm^{-1} to 7.6804 cm^{-1} .

The isotopic shifts due to the deuterium substitution are listed and compared with other similar substitution in Table 11.

Table 11

Isotopic Shifts of C-O bands for Deuterium Substitution

Compounds	Isotopic Shifts (cm^{-1})	Ref.
CH_3CHO and CH_3CDO	63.4	This work
CD_3CHO and CD_3CDO	40	This work
$C_2H_2O_2$ and C_2HDO_2	20	(22)
$H_2C=CH-CHO$ and $H_2C=CH-CDO$	30	(23)
$HC\equiv C-CHO$ and $HC\equiv C-CDO$	43.6	(24)
$DC\equiv C-CHO$ and $DC\equiv C-CDO$	43.69	(24)
CH_3CDO and CD_3CDO	7.2	This work
CH_3CHO and CD_3CHO	16.7	This work
$(CH_3CO)_2$ and $(CD_3CO)_2$	23	(25)
H_2CO and D_2CO	113	(26)

The shift for CH_3CHO and CH_3CDO was expected to be equal to the shift for CD_3CHO and CD_3CDO, and similarly, the shift for CH_3CDO and CD_3CDO would equal to for CH_3CHO and CD_3CHO, because the values were obtained from the same type of substitution. In Table 11, the shift for CD_3CHO and CD_3CDO was in agreement with the values from the other compounds, but the shift for CH_3CHO and CH_3CDO was found to have a much larger value. The shift for CH_3CDO and CD_3CDO was in agreement with the value for $(CH_3CO)_2$ and $(CD_3CO)_2$. It suggested that the O-O band of CH_3CHO was in error by 10 cm^{-1}. The comparisons for the observed and calcualted band patterns, which were based on the origin at 27683 cm^{-1}, were found not to be in agreement with the result of the least squares fit programme. If a better comparison was found between the observed and the calculated band patterns, it might improve the refined value of the O-O band position of CH_3CHO, and the shifts between the above two sets of compounds would be nearly equal.

The unassigned transitions in the spectrum of CH_3CHO might be related to the progressions which were formed by the transitions between the vibrationally induced electronic states. From the irregularity of the energy spacings of these progressions, it was suggested that the selection rules of the transitions might be different from those for the allowed electronic transitions.

Future detailed studies of these progressions would be of great value in confirming the true position of the 0-0 band of acetaldehyde and the assignment of perturbing vibration.

REFERENCE

1. G. Herzberg , " Molecular Spectra and Molecular Structure : Vol. III , Electronic Spectra and Electronic Structure of Polyatomic Molecules " , D. Van Nostrand Company , Inc., Princeton, New York (1966)
2. V. Henri and S. A. Schou , Z. Physik 49 , 774 (1928)
3. P. A. Leighton and F. E. Blacet , J. Amer. Chem. Soc., 55 , 1766 (1933)
4. S. A. Schou , J. Chim. Phys. 26 , 27 (1929)
5. V. R. Rao and I. A. Rao , Ind. J. Phys. 28 , 491 (1954)
6. K. K. Innes and L. E. Giddings Jr., J. Mol. Spect. 7 , 435 (1961)
7. E. Murad , J. Phys. Chem. 64 , 942 (1960)
8. E. F. Worden Jr., Spect. Acta 22 , 21 (1966)
9. W. G. Fateley and F. A. Miller , Spect. Acta 17 , 857 (1961)
10. R. W. Kilb , C. C. Lin and E. B. Wilson Jr., J. Chem. Phys., 26 (6) , 1965 (1957)
11. C. E. Souter and J. L. Wood , J. Chem. Phys., 52 (2) , 674 (1968)
12. D. R. Herschbach, J. Chem. Phys., 31 (1) , 91 (1959)
13. J. D. Lewis , T. B. Malloy Jr., T. H. Chao and J. Laane , J. Mole. Structure 12 , 427 (1972)
14. R. D. Gorden , S. C. Dass , J. R. Robins , H. F. Shurvell and R. F. Whitlock , Can. J. Chem. 54 , 2658 (1976)
15. J. R. Durig , S. M. Craven and W. C. Harris , " Vibrational Spectra and Structure : Vol. 1 , Chapter 4 , Determination of Torsional Barriers from Far-Infrared Spectra. " , Marcel Dekker Inc., New York , 1972

16. J. U. White , J. Opt. Soc. Am. 32 , 285 (1942)

17. A. Biernacki , D. C. Moule and J. L. Neale , Applied Spect. 26(6), 648 (1972)

18. M. S. Matheson and J. W. Zabor , J. Chem. Phys. 7 , 536 (1939)

19. H. M. Crosswhite , J. of Research of the National Bureau of Standards - A Physics and Chemistry , Vol. 79 A , No. 1 , Jan-Feb. 1975 ,pp.17

20. N. R. C. table , Internal Report , National Research Council of Canada , Ottawa , Ontario .

21. D. R. Herschbach , " Tables for the Internal Rotation Problem " , Dept. of Chemistry , Harvard University.

22. J. Paldus and D. A. Ramsay , Can. J. Phys. , Vol. 45 , 1389 (1967)

23. C. D. Brand and D. G. Williamson , " The Structure of Electronically Excited Species in the Gas-Phase -- A General Discussion of The Faraday Society , No. 35 , 1963. ' Near-Ultraviolet Spectrum of Propenal ' " , The Aberdeen University Press Ltd., Scotland

24. J. C. D. Brand, W. H. Chan, and D. S. Liu, J. Mol. Spect. 50, 304 (1974)

25. J. W. Sidman and D. S. McClure , J. Am. Chem. Soc., 77 , 6461 (1955)

26. V. A. Job , V. Sethuraman , and K. K. Innes , J. Mol. Spect. 30 , No. 3 , 365 (1969)

27. H. C. Allen, Jr. and P. C. Cross , " Molecular Vib-Rotors, Chapter 2 , P.24, " John Wiley and Sons, Inc.,New York, 1963

28. J. A. Pople and D. L. Beveridge " Approximate Molecular Orbital Theory " , McGraw-Hill Book Company, New York, 1970